Journal of Magnetic Resonance 349 (2023) 107410

Contents lists available at ScienceDirect

Journal of Magnetic Resonance

journal homepage: www.elsevier.com/locate/jmr

Computational tools for the simulation and analysis of spin-polarized EPR spectra

Claudia E. Tait [a,*], Matthew D. Krzyaniak [b], Stefan Stoll [c]

[a] Department of Chemistry, University of Oxford, Oxford OX1 3QZ, United Kingdom
[b] Department of Chemistry, Center for Molecular Quantum Transduction and Institute for Sustainability and Energy at Northwestern, Northwestern University, Evanston 60208, IL, United States
[c] Department of Chemistry, University of Washington, Seattle, 98195, WA, United States

ARTICLE INFO

Article history:
Received 23 December 2022
Revised 10 February 2023
Accepted 18 February 2023
Available online 24 February 2023

Keywords:
Electron spin polarization
Transient EPR
Time-resolved ESR
Photoexcited triplet state
Spin-correlated radical pair
Intersystem crossing
Singlet fission
Spin qubit

ABSTRACT

The EPR spectra of paramagnetic species induced by photoexcitation typically exhibit enhanced absorptive and emissive features resulting from sublevel populations that differ from thermal equilibrium. The populations and the resulting spin polarization of the spectra are dictated by the selectivity of the photophysical process generating the observed state. Simulation of the spin-polarized EPR spectra is crucial in the characterization of both the dynamics of formation of the photoexcited state as well as its electronic and structural properties. EasySpin, the simulation toolbox for EPR spectroscopy, now includes extended support for the simulation of the EPR spectra of spin-polarized states of arbitrary spin multiplicity and formed by a variety of different mechanisms, including photoexcited triplet states populated by intersystem crossing, charge recombination or spin polarization transfer, spin-correlated radical pairs created by photoinduced electron transfer, triplet pairs formed by singlet fission and multiplet states arising from photoexcitation in systems containing chromophores and stable radicals. In this paper, we highlight EasySpin's capabilities for the simulation of spin-polarized EPR spectra on the basis of illustrative examples from the literature in a variety of fields ranging across chemistry, biology, material science and quantum information science.

1. Introduction

Spin-polarized systems have long held a fascination within the field of Electron Paramagnetic Resonance (EPR) spectroscopy as, in addition to the magnetic parameters characterizing the spin system, a spin-polarized EPR spectrum also contains information on the dynamics that have led to the formation of the observed paramagnetic state. Spin polarization refers to a non-Boltzmann distribution of spin sublevel populations and arises due to the spin selectivity of processes generating paramagnetic species, most commonly from a photoexcited precursor, including intersystem crossing (ISC), energy transfer and electron transfer processes. Spin polarization typically also leads to significantly enhanced EPR intensities and improved sensitivity.

Early studies on spin-polarized systems focused on photoexcited triplet states of organic molecules in crystals and rigid glasses [1,2] and organic radicals formed by photolysis in solution [3]. Additionally, the investigation of spin-correlated radical pairs and triplet states in photosynthetic reaction centres and model systems contributed significantly to the understanding of the photosynthetic mechanism [4–11] and the study of light-induced electron transfer in cryptochrome and photolyase proteins is still shedding light on the role of spin-correlated radical pairs in a variety of biological processes [12,13]. More recently, EPR on spin-polarized systems has gained increasing importance in materials science with investigations of charge separation mechanisms in organic photovoltaics [14–17], triplet pair formation by singlet fission [18–20] and thermally activated delayed fluorescence (TADF) in materials for organic light-emitting diodes (OLEDs) [21–23]. Spin-polarized triplet states have also been proposed as spin labels to increase sensitivity in dipolar EPR for the investigation of structure and dynamics of proteins [24–27]. Photogenerated spin-polarized states are also gaining interest as spin qubits for quantum information science [28–32].

The EPR technique of choice for the investigation of spin-polarized systems is transient or time-resolved EPR, a continuous-wave EPR technique based on the measurement of microwave absorption as a function of time after photoexcitation

* Corresponding author.
E-mail address: claudia.tait@chem.ox.ac.uk (C.E. Tait).

https://doi.org/10.1016/j.jmr.2023.107410
1090-7807/

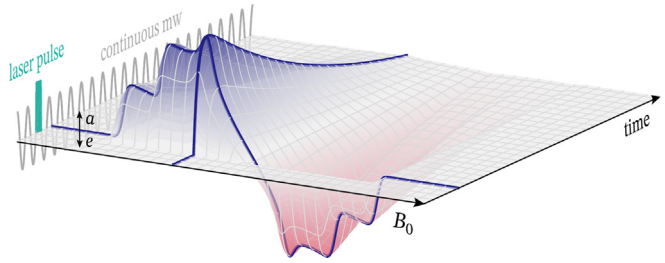

Fig. 1. Schematic illustration of the transient EPR experiment: The EPR signal is detected as a function of time after photoexcitation with a laser pulse under continuous microwave irradiation at each magnetic field position (*a* = absorption, *e* = emission). A transient illustrating the time dependence at a single field position and the EPR spectrum at a fixed time after photoexcitation are highlighted.

and as a function of magnetic field (Fig. 1). Time-resolved spectral information is obtained by extracting slices at different times after photoexcitation and kinetic information can be obtained from transients at selected field positions. The technical implementation of transient EPR and important experimental considerations are comprehensively reviewed in references [33,34].

Experimental studies of spin-polarized systems by transient EPR are often complemented by pulse EPR measurements to provide more detailed information, e.g. time-resolved ENDOR, ESEEM and HYSCORE for the measurement of hyperfine couplings [35–38], out-of-phase ESEEM on spin-correlated radical pairs for the precise characterization of the dipolar and exchange interactions [39,40], pulse sequences for the investigation of dynamical processes [35,41], and nutation experiments for the separation of contributions from states with different spin multiplicities [42,18,31]. Simulation of a variety of pulse EPR experiments is possible in EasySpin [43] and can be used for photoexcited states, but will not be discussed here.

The interpretation of the observed spectral shapes and spin polarizations in terms of electronic and molecular structures as well as dynamics of formation of the paramagnetic state generally requires computational modeling for the extraction of magnetic parameters and population distributions. However, most available EPR simulation packages include, if any, only limited support for the simulation of the EPR spectra of spin-polarized states. Several research groups have developed their own simulation approaches and code for spin-polarized systems [44–59], but these tend to be tailored to specific types of spin-polarized systems of interest to the group and are not always easily accessible by the wider research community. Here we report on an extension of EasySpin [60], a widely used open-source MATLAB toolbox for simulation and fitting of EPR spectra, to provide improved simulation capabilities for spin-polarized systems.

A general implementation of the calculation of the polarization of individual transitions resulting from non-Boltzmann population of the spin sublevels and a flexible interface allow simulations for a wide range of spin systems (triplets, radical pairs, quartet states, triplet pairs, etc.) and different spin polarization mechanisms (e.g. ISC, energy transfer, photoinduced charge separation and recombination, singlet fission). In addition to providing a general and user-friendly simulation tool for spin-polarized systems, this approach also takes advantage of EasySpin's efficient and accurate spectral simulation and fitting algorithms [60]. The extended capabilities for simulation of spin-polarized systems are included starting from version 6.0 of EasySpin, available online at easyspin.org. In this paper, we describe and demonstrate EasySpin's simulation capabilities for spin-polarized systems based on a series of illustrative examples from the literature.

2. Simulation of spin-polarized EPR spectra

The spin polarization observed in EPR spectra of photoexcited states results from an initial state of the spin system that differs from the Boltzmann thermal equilibrium population of the spin sublevels. The intensity of an EPR transition between the states *i* and *j* is determined by the transition rate and the population difference between those states [60]

$$I_{ij}^{\mathrm{EPR}} \propto \left|\left\langle i\middle|\boldsymbol{B}_1^{\mathrm{T}}\hat{\boldsymbol{\mu}}\middle|j\right\rangle\right|^2 (p_i - p_j) \tag{1}$$

where $\boldsymbol{B}_1$ is the microwave magnetic field component vector, $\hat{\boldsymbol{\mu}}$ is the magnetic dipole moment operator of the spin system, and p_i and p_j are the populations of the two eigenstates $|\,i\rangle$ and $|\,j\rangle$ involved in the transition. These populations are given by the corresponding diagonal element of the density matrix in the eigenframe of the spin Hamiltonian.

$$p_i = \langle i\,|\,\hat{\rho}\,|\,i\rangle = \rho_{ii,\mathrm{eig}} \tag{2}$$

Different spin polarization mechanisms lead to different population distributions and, depending on the exact mechanism, are generally most conveniently expressed in a specific basis that might differ from the eigenbasis or the uncoupled basis used in EasySpin to set up the spin Hamiltonian and perform calculations. In some cases, the initial state of a photoexcited species is most conveniently defined in terms of the populations of the basis states of the precursor, corresponding to an initial density matrix

$$\hat{\rho} = \sum_i p_i\,|\,i\rangle\langle i\,| \tag{3}$$

EasySpin now allows the definition of non-equilibrium initial states when simulating solid-state spectra using the function `pepper`. The initial state of the spin system can be specified in a range of different bases using the `initState` field in the spin system structure with the syntax `Sys.initState = {state,basis}`, where `state` corresponds to the initial state and `basis` is a keyword specifying the corresponding basis. The initial state can be defined in terms of a list of populations, for example p_X, p_Y and p_Z for a triplet state, or the full density matrix, for example $\hat{\rho} = |\,S\rangle\langle S\,|$ for a singlet-born radical pair. The bases available for the definition of the initial state are:

- the uncoupled product Zeeman basis, $|\,m_{s,1}, m_{s,2}, \ldots\rangle$, in order of descending $m_{s,i}$ (`'uncoupled'`),
- the coupled basis for a system of two coupled spins, $|\,S_{\mathrm{tot}}, m_{S,\mathrm{tot}}\rangle$, in order of descending S_{tot} and, for each value of S_{tot}, in descending order of $m_{S,\mathrm{tot}}$ (`'coupled'`),
- the eigenbasis of the full spin Hamiltonian, with eigenstates in order of increasing energy[1] (`'eigen'`),
- the eigenbasis of the spin Hamiltonian at zero field, with eigenstates ordered in terms of increasing energy (`'zerofield'`),
- the $|\,T_X\rangle, |\,T_Y\rangle, |\,T_Z\rangle$ basis for a triplet state (`'xyz'`)

$$\begin{aligned} |\,T_X\rangle &= \tfrac{1}{\sqrt{2}}(|\,T_{+1}\rangle - |\,T_{-1}\rangle) \\ |\,T_Y\rangle &= \tfrac{1}{\sqrt{2}}(|\,T_{+1}\rangle + |\,T_{-1}\rangle) \\ |\,T_Z\rangle &= |\,T_0\rangle \end{aligned} \tag{4}$$

EasySpin internally converts the `Sys.initState` input to a density matrix in the uncoupled basis and uses Eq. 2 to calculate sublevel populations.

[1] When defining the initial state in terms of populations of the eigenstates of the system, care must be taken that the spin character of the energy-ordered eigenstates is maintained for varying orientations, which is not the case in some instances for spin systems of weakly to moderately coupled spins.

In the following, we describe the main spin polarization mechanisms and show examples from the literature using spectra simulated with EasySpin. We start by discussing spin polarization in triplet and quartet states formed by intersystem crossing from a photoexcited state of different spin multiplicity, followed by a discussion of the transfer of spin polarization between states of the same multiplicity. Spin-polarized states arising as a consequence of photoinduced electron transfer, such as spin-correlated radical pairs and triplet states formed by recombination, are covered in the section on electron transfer processes. Finally, the simulation of spin-polarized EPR spectra resulting from singlet fission are discussed. This is followed by a description of the simulation of photoselection effects for photoexcitation with linearly polarized light and of partial ordering effects in samples where the photoexcited states assume preferential orientations with respect to the magnetic field. We conclude with a section on modeling of the time evolution of spin polarizations as a consequence of simple spin-selective dynamics. The simulation scripts for all of the examples are included in the SI.

3. Intersystem crossing

Intersystem crossing processes describe a conversion between states of different spin multiplicity, which is generally driven by direct spin–orbit coupling or through a spin–vibronic mechanism involving state mixing by simultaneous vibronic and spin–orbit coupling [61]. The required change in spin angular momentum is compensated by an opposite change in orbital angular momentum, and since changes in orbital angular momentum are more likely along some directions in the molecular frame, this results in anisotropic ISC rates and selective population of the spin sublevels in the molecular frame [62].

In systems of coupled unlike electron spins, conversion between states of different spin multiplicity can also be mediated by differences in electron Zeeman interactions of the coupled spins (Δg mechanism) or by different hyperfine interactions experienced by the spins [63]. This process is generally referred to as singlet–triplet mixing or radical pair intersystem crossing (RP-ISC) and will be discussed in more detail in the section on electron transfer processes.

3.1. Triplet states generated by spin–orbit ISC

Intersystem crossing from an excited singlet state to a triplet state results in selective population of the T_X, T_Y and T_Z triplet state sublevels, defined with respect to the molecular frame (see Fig. 2).

The EPR spectrum of a triplet state arises from the transitions between the triplet eigenstates $T_{-1} \leftrightarrow T_0$ and $T_0 \leftrightarrow T_{+1}$, at energies determined by the spin Hamiltonian (in frequency units)

$$\hat{\mathscr{H}} = \frac{\mu_B}{h}\boldsymbol{B}_0^T\boldsymbol{g}\hat{\boldsymbol{S}} + \hat{\boldsymbol{S}}^T\boldsymbol{D}\hat{\boldsymbol{S}} \tag{5}$$

where the first term describes the electron Zeeman interaction and the second one the zero-field (ZF) interaction. The zero-field interaction matrix $\boldsymbol{D}$ is usually set to be traceless and characterized by the parameters D and E defined in terms of the principal values D_X, D_Y and D_Z as follows

$$D = \frac{3}{2}D_Z \qquad E = \frac{1}{2}(D_X - D_Y) \tag{6}$$

where $|D| > 3|E|$ by convention. For organic triplet states, there is the additional convention to assign the axis labels X,Y and Z such that $|D_Z| > |D_X| > |D_Y|$ and therefore $-\frac{1}{3} \leqslant E/D \leq 0$ [66].

The magnitude of D and E can be determined from the positions of the turning points in the triplet spectrum, however the sign of D is typically not directly evident from the EPR spectrum and its determination requires more advanced measurement approaches or measurements at low temperatures and high fields [38]. In organic systems, where the ZF interaction is mainly determined by spin–spin coupling, the magnitude of D depends on the inter-spin distance averaged over the triplet wavefunction and the sign is determined by the symmetry of the spin density distribution, with $D < 0$ for prolate and $D > 0$ for oblate distributions. The signs of D and E determine the level ordering of the T_X, T_Y and T_Z states at zero field:

$$\begin{aligned} E_X &= \tfrac{1}{3}D - E \\ E_Y &= \tfrac{1}{3}D + E \\ E_Z &= -\tfrac{2}{3}D \end{aligned} \tag{7}$$

The spin polarization pattern of the EPR spectra of photoexcited triplet states is determined by the selectivity of the ISC mechanism in populating the T_X, T_Y and T_Z states, which results in orientation-dependent population of the T_{-1}, T_0 and T_{+1} states [67]. For an applied magnetic field $\boldsymbol{B}_0$ aligned with one of the principal axes of the zero-field interaction matrix, the populations of the T_{-1}, T_0 and T_{+1} states are given by

$$\boldsymbol{B}_0 \| \boldsymbol{i}: \quad p_0 = p_i \qquad p_{\pm 1} = \frac{1}{2}(p_j + p_k) \tag{8}$$

where i corresponds to the principal axis aligned with $\boldsymbol{B}_0$ (e.g. X) and j and k correspond to the other two axes (e.g. Y and Z).

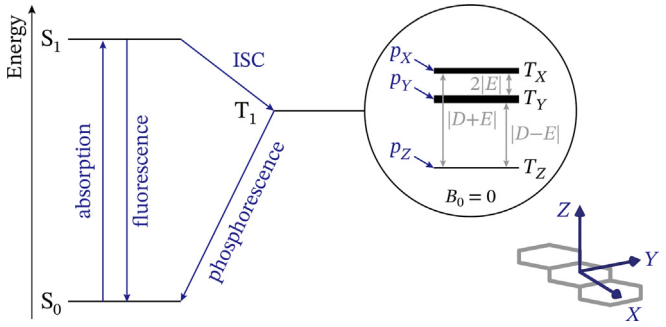

Fig. 2. Energy level diagram illustrating the photophysical processes occurring upon photoexcitation of a molecule in a singlet ground state. Intersystem crossing selectively populates the triplet sublevels T_X, T_Y and T_Z associated with the molecule-fixed principal axes of the zero-field interaction matrix.

Fig. 3 illustrates the origin of the observed spectral shape and spin polarization pattern of a photoexcited triplet state populated by ISC on the example of anthracene. The absence of heavy nuclei results in only small direct spin–orbit coupling contributions and therefore ISC in anthracene, and other planar polycyclic hydrocarbons, is driven by vibrational spin–orbit coupling and leads to selective population of the in-plane triplet sublevels, T_X and T_Y [65,68]. The energy level diagrams for a magnetic field aligned with each of the ZF principal axes in Fig. 3 show how this selective population of T_X and T_Y leads to an overall *eeeaaa* polarization pattern of the triplet state EPR spectrum. In addition to the allowed $\Delta m_S = \pm 1$ transitions, the formally forbidden double-quantum transition ($\Delta m_S = \pm 2$) also contributes to the spectrum at half-field.

Simulation of spin-polarized EPR spectra allows extraction of the zero-field D and E parameters, reflecting the extent and symmetry of the spin density distribution, and of the relative sublevel populations, revealing insights into the nature of the ISC mechanism. In EasySpin, the EPR spectra of photoexcited triplet states resulting from ISC can be simulated by providing the ZF parameters and defining the initial state in terms of the populations in the T_X, T_Y, T_Z basis as `Sys.initState = {[px py pz],'xyz'}`. In the following examples, the ZF parameters and sublevel popula-

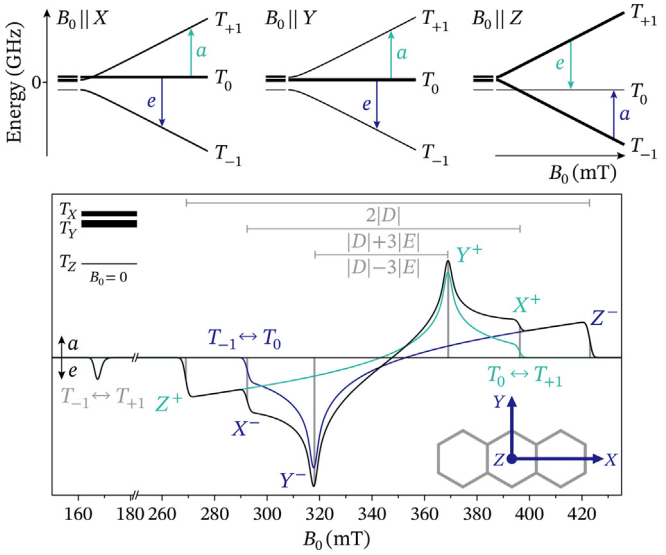

Fig. 3. EPR spectrum of the anthracene triplet state formed by ISC and energies of the triplet sublevels as a function of an applied magnetic field oriented parallel to the principal axes of the ZF interaction matrix. The spectrum was simulated with ZF interaction parameters D = +2159 MHz and E = -246 MHz [64] and relative sublevel populations $p_X : p_Y : p_Z = 1 : 1.4 : 0.14$ [65] (see `SOISC_triplet_Ant.m` in the SI). The contributions of the $m_S = -1 \leftrightarrow m_S = 0$ and $m_S = 0 \leftrightarrow m_S = +1$ transitions to the spectrum are shown in blue and green, respectively. The six canonical transitions and the $\Delta m_S = \pm 2$ transition at half-field are highlighted. The insets show the distribution of the populations across the T_X, T_Y and T_Z sublevels and the orientation of the principal axes of the ZF interaction matrix with respect to the molecular structure.

tions leading to the observed spin polarizations are pictorially summarized by an energy level diagram of the T_X, T_Y and T_Z states at zero field with line thicknesses representing the corresponding population distribution $p_X : p_Y : p_Z$.

The example in Fig. 4 illustrates how changes in the extent of spin density delocalization affect the triplet state EPR spectrum for a zinc porphyrin monomer and the corresponding butadiyne-linked dimer. The zinc porphyrin monomer spectrum exhibits an *aaaeee* spin polarization resulting from predominant population of the T_Z, out-of-plane, triplet sublevel due to ISC driven by direct spin–orbit coupling of the heavy Zn nucleus. The triplet EPR spectrum of the porphyrin dimer is characterized by a significantly different spin polarization pattern, *aaeaee*, indicative of preferential population of the T_X sublevel. The differences between monomer and dimer triplet spectra are due to a shift of the axis of maximum dipolar coupling, associated with the T_Z sublevel, from the out-of-plane axis in the porphyrin monomer to the long in-plane axis in the dimer as a result of spin density delocalization over both porphyrin units [69]. This delocalization leads to a change from an oblate to a prolate spin density distribution and an associated change in the sign of D. ISC is still driven by direct spin–orbit coupling and selectively populates the out-of-plane sublevel, which in the dimer corresponds to T_X, resulting in the observed spin polarization.

Differences in the spin polarization pattern for triplet states in related molecules can sometimes reveal aspects of the nature of the photoexcited state and the dynamics of its formation not accessible by other techniques. This is illustrated in the example of Fig. 5, where the triplet state EPR spectra of anthracene and dimethyljulolidine (DMJ)-anthracene are compared. The similar positions of the six canonical transitions and therefore similar ZF parameters indicate that the triplet state is localized on anthracene for both molecules. The change in spin polarization from the characteristic *eeeaaa* pattern of anthracene to *eaeaea* for DMJ-anthracene is due to preferential population of the T_Y sublevel in the latter, which results from ISC driven by a spin–orbit mechanism coupling a photoinduced charge transfer state to the triplet state and referred to as spin–orbit charge-transfer intersystem crossing (SOCT-ISC) [70,71]. This mechanism is active in systems where charge transfer is accompanied by a significant change in orbital angular momentum, e.g. systems with perpendicular arrangement of the donor and acceptor molecular orbitals. In DMJ-anthracene, the charge transfer between the approximately perpendicular π systems of DMJ and anthracene involves an orbital angular momentum change along the principal axis associated with the T_Y sublevel and therefore SOCT-ISC preferentially populates this sublevel [70].

3.2. ISC crossing in coupled triplet–radical systems

The EPR spectra of photoexcited multiplet species with overall spin $S > 1$, for example coupled photoexcited triplet and radical states, show similarities to those of photoexcited triplet states and can similarly be simulated in EasySpin to extract interaction parameters and population distributions to reveal information on the structure and extent of spin density distribution and on the photophysics of the system.

The Hamiltonian for a system of a triplet state ($S_T = 1$) coupled to a doublet (radical) state ($S_R = \frac{1}{2}$) is given by

$$\hat{\mathscr{H}} = \frac{\mu_B}{h}\mathbf{B}_0^T\mathbf{g}_T\hat{\mathbf{S}}_T + \frac{\mu_B}{h}\mathbf{B}_0^T\mathbf{g}_R\hat{\mathbf{S}}_R + \hat{\mathbf{S}}_T^T\mathbf{D}_T\hat{\mathbf{S}}_T + \hat{\mathbf{S}}_T^T\mathbf{D}_{TR}\hat{\mathbf{S}}_R + J_{TR}\hat{\mathbf{S}}_T^T\hat{\mathbf{S}}_R \quad (9)$$

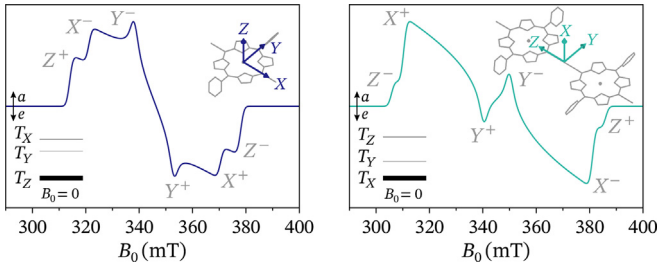

Fig. 4. EPR spectra of the photoexcited triplet states of a zinc porphyrin monomer and butadiyne-linked zinc porphyrin dimer formed by ISC. The porphyrin monomer spectrum was simulated with D = +898 MHz, E = -161 MHz, $p_X : p_Y : p_Z = 0.05 : 0 : 0.95$ and the dimer spectrum with D = -1125 MHz, E = 285 MHz, $p_X : p_Y : p_Z = 0.94 : 0 : 0.06$ [69] (see script `SOISC_triplet_ZnP.m` in the SI). The insets show the orientation of the ZF frames with respect to the molecular structure.

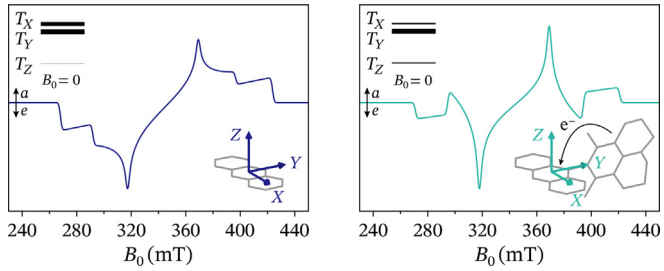

Fig. 5. EPR spectra of the photoexcited triplet state of anthracene formed by ISC and of the triplet state of dimethyljulolidine (DMJ)-anthracene formed by spin–orbit charge-transfer (SOCT) ISC. The spectra were simulated with D = +2181 MHz, E = -247 MHz, $p_X : p_Y : p_Z = 0.78 : 1 : 0.07$ for anthracene and D = +2101 MHz, E = -225 MHz, $p_X : p_Y : p_Z = 0.26 : 1 : 0.21$ for DMJ-anthracene [70] (see script `SOCTISC_triplet_DMJAnt.m` in the SI).

Depending on the strength of the exchange interaction, J_{TR}, the system is best modeled either as a quartet state with effective g-values and ZF interactions [48,72] or as a coupled triplet–doublet pair for the purpose of simulation of the EPR spectrum [73]. In the strong exchange coupling limit, when the exchange interaction significantly exceeds any other interactions present, the system can be described in terms of a combination of an excited doublet ($S = \frac{1}{2}$) state and a quartet state ($S = \frac{3}{2}$), and the zero-field interaction in the quartet state is determined by the zero-field interaction in the triplet state, $\boldsymbol{D}_T$ and the dipole–dipole interaction between the triplet state and the radical, $\boldsymbol{D}_{TR}$,[2] as [48,72]

$$\boldsymbol{D}_Q = \frac{1}{3}(\boldsymbol{D}_T + \boldsymbol{D}_{TR}) \tag{10}$$

The polarization patterns of quartet species are also determined by spin–orbit-driven ISC with a selectivity following the molecular symmetry, and are most conveniently defined in terms of population distributions in a basis associated with the molecular frame, i.e. the zero-field eigenbasis. The quartet states can be expressed in terms of the states of the constituent triplet and radical as [74]

$$\begin{aligned} |\pm\tfrac{3}{2}\rangle &= |T_{\pm1}R_{\pm}\rangle \\ |\pm\tfrac{1}{2}\rangle &= \tfrac{1}{\sqrt{3}}(|T_{\pm1}R_{\mp}\rangle + \sqrt{2}\,|T_0R_{\pm}\rangle) \end{aligned} \tag{11}$$

where R_+ and R_- refer to the radical α and β states and the triplet T_{-1}, T_0 and T_{+1} states are related to the T_X, T_Y and T_Z states as described in Eq. 4. Assuming collinear ZF principal axis systems of the triplet and quartet states, the corresponding populations can be derived as follows [74]

$$\begin{aligned} p_{\pm3/2} &\propto \tfrac{1}{2}(p_X + p_Y) \\ p_{\pm1/2} &\propto \tfrac{2}{3}p_Z + \tfrac{1}{6}(p_X + p_Y) \end{aligned} \tag{12}$$

In EasySpin, spin-polarized spectra of quartet states formed by ISC can be simulated by calculating the initial density matrix from the states and populations given in Eq. 11 and Eq. 12 as shown in the code associated with the following example.[3] Alternatively, the system can be simulated explicitly for a coupled triplet and radical state, with an initial density matrix constructed as the Kronecker product of the respective triplet and radical density matrices.

The example in Fig. 6 compares the EPR spectra of the photoexcited triplet states of phthalocyanines with a Zn or Mg central metal to the spectra of the quartet states observed in the presence of a coordinated TEMPO radical [74] to illustrate the parallels between ISC-populated triplet and quartet states and the corresponding simulation approaches. The opposite spin polarization patterns for the triplet states of ZnPc and MgPc arise from differences in the ISC mechanism, with the direct spin–orbit coupling contribution preferentially populating the out-of-plane T_Z sublevel for the heavier ZnPc, whereas in MgPc ISC is driven by vibronic coupling and preferentially populates the in-plane sublevels T_X and T_Y.

The photoexcited EPR spectra of the corresponding phthalocyanines with a coordinated TEMPO radical are significantly narrower, as these strongly coupled systems can be described as quartet states with zero-field interactions related to the ones in the corresponding triplet states as described in Eq. 10. In analogy to the corresponding triplet states, the opposite spin polarization patterns for ZnPc-TEMPO• and MgPc-TEMPO• are determined by sublevel-

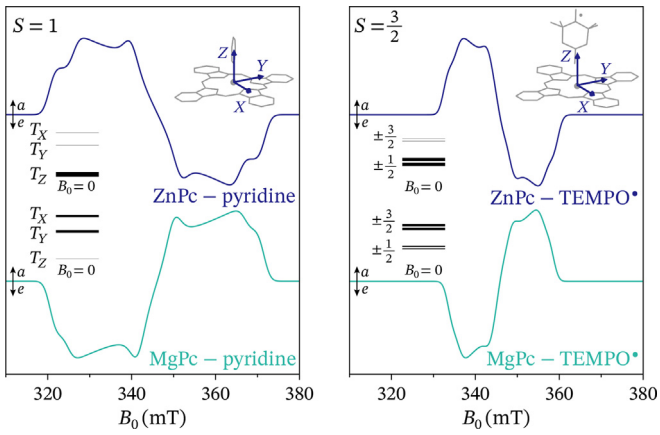

Fig. 6. Triplet state EPR spectra of Zn and Mg phthalocyanine (Pc) and quartet state EPR spectra of the same compounds with TEMPO coordinated to the central metal instead of pyridine. The triplet spectra were simulated with D = 720 MHz, E = -130 MHz, $p_X : p_Y : p_Z = 0 : 0 : 1$ for ZnPc and D = 713 MHz, E = -157 MHz, $p_X : p_Y : p_Z = 0.46 : 0.54 : 0$ for MgPc, the quartet spectra were simulated with D = 190 MHz, E = -35 MHz, $p_{\pm1/2} : p_{\pm3/2} = 0.67 : 0$ for ZnPc-TEMPO• and D = 175 MHz, E = -35 MHz, $p_{\pm1/2} : p_{\pm3/2} = 0.17 : 0.50$ for MgPc-TEMPO• [74] (see script `SOISC_quartet_PcTEMPO.m` in the SI).

selective ISC between the excited doublet and quartet states. Due to symmetry, ISC equally populates the $\pm\frac{3}{2}$ states, and similarly the $\pm\frac{1}{2}$ states [52]. The spin polarization pattern of ZnPc-TEMPO• arises from selective population of the quartet $m_S = \pm\frac{1}{2}$ states due to the out-of-plane component of spin–orbit coupling, whereas in-plane components selectively populate the $m_S = \pm\frac{3}{2}$ states in MgPc-TEMPO• [74].

Experimental EPR spectra of systems with coupled triplet and doublet states are often also characterized by a narrow component with net polarization at the center of the spectrum in addition to the multiplet polarization reminiscent of the spectra of photoexcited triplet states. This net polarization arises in part from population of the quartet state by spin–orbit-driven intersystem crossing and will therefore be included in simulations following the approach described so far, but may be masked by additional contributions of spin-polarized excited- or ground-state doublet species or arising from other population mechanisms that would have to be simulated as additional contributions [52,48].

A different type of spin polarization pattern of systems containing a stable radical in the vicinity of a photoexcited chromophore can result from enhanced intersystem crossing (EISC) induced by electron exchange coupling, which is generally much faster than typical spin–orbit ISC [75]. The enhancement depends strongly on the overlap of the wavefunctions of the photoexcited chromophore and radical and on the energy difference between the chromophore excited singlet and triplet states [76]. Since the exchange interaction driving this type of ISC is isotropic, EISC does not depend on molecular symmetry and the population distribution in the excited state is governed by spin conservation, leading to the population of the $m_s = \pm\frac{1}{2}$ sublevels of the coupled doublet–triplet system from the doublet excited state independent of orientation [75] (Fig. 7). Simulations of the resulting spin-polarized EPR spectra can be performed based on the populations of the high-field eigenstates of the spin Hamiltonian as `Sys.initState = {pvector,'eigen'}`.

An example of a spin-polarized EPR spectrum of a quartet state formed by EISC is shown in Fig. 7 for a substituted perylenediimide (PDI) covalently linked to a TEMPO• radical [31]. The observed *aeeaae* polarization pattern of the $|\pm\frac{3}{2}\rangle \leftrightarrow |\pm\frac{1}{2}\rangle$ transitions cannot be reproduced by considering spin–orbit-driven ISC

[2] In this article, $\boldsymbol{D}$ is used both for zero-field interaction matrices as well as dipole–dipole interaction matrices, the corresponding terms in the spin Hamiltonian are written as $\hat{\boldsymbol{S}}^T\boldsymbol{D}\hat{\boldsymbol{S}}$ for the former and $\hat{\boldsymbol{S}}_A^T\boldsymbol{D}_{AB}\hat{\boldsymbol{S}}_B$ for the latter.

[3] The definition of the non-equilibrium population of a photoexcited quartet state in the zero-field eigenbasis of `Sys.initState` is ambiguous due to the degeneracy of the $\pm\frac{1}{2}$ and $\pm\frac{3}{2}$ states, therefore the full initial density matrix should be calculated and provided as input.

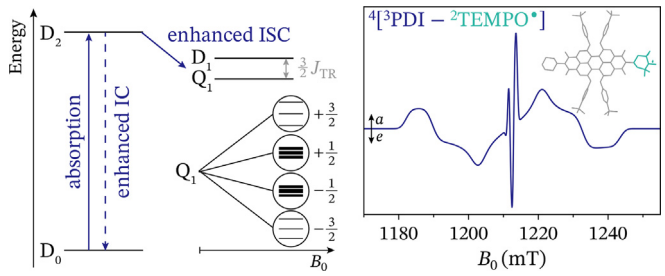

Fig. 7. Schematic illustration of the enhanced ISC process in a system of a chromophore coupled to a stable radical, population distribution in the high-field eigenstates and Q-band EPR spectrum of the photoexcited quartet state of a substituted perylene-diimide (PDI) covalently linked to TEMPO• populated by EISC. The spectrum was simulated as a quartet ($S = \frac{3}{2}$) state with g-values of 2.0057, 2.0045 and 2.0030, ZF interaction parameters D = 430 MHz and E = -60 MHz, hyperfine coupling to a ^{14}N nucleus with $A_\perp$ = 6.3 MHz and $A_\parallel$ = 32 MHz and populations of 0 : 0 : 0 : 0.15 : 0.20 : 0.16 : 0.10 : 0.27 : 0.13 : 0 : 0 : 0 for the energy-ordered eigenstates at high field [31] (see script `EISC_quartet_PDITEMPO.m` in the SI).

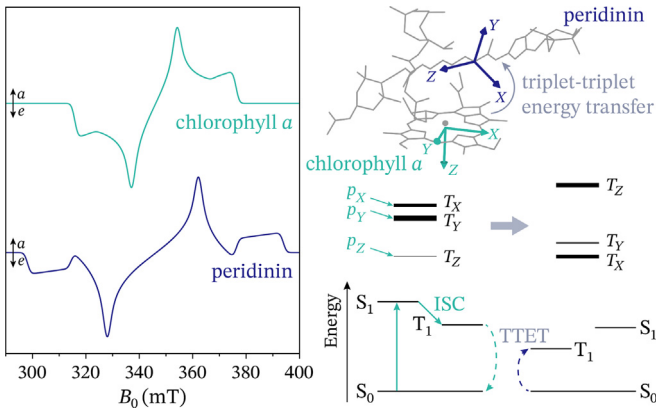

Fig. 8. EPR spectra of the photoexcited triplet state of chlorophyll *a* formed by ISC and of the excited triplet state of peridinin formed by triplet–triplet energy transfer from a chlorophyll *a* molecule in the peridinin-chlorophyll *a*-protein, a light-harvesting complex of dinoflagellates. The relative orientation of the pair of chlorophyll and peridinin molecules involved in TTET in PCP [83] and of the corresponding ZF interaction frames are shown as well as the population distribution among the T_X, T_Y and T_Z sublevels. The triplet spectrum of chlorophyll *a* was simulated with ZF interaction parameters D = 846 MHz and E = -123 MHz and sublevel populations $p_X : p_Y : p_Z = 0.33 : 0.56 : 0.11$, the triplet spectrum of peridinin with D = -1342 MHz and E = 129 MHz and sublevel populations $p_X : p_Y : p_Z = 0.39 : 0.14 : 0.47$ [82] (see script `TTET_triplet_PCP.m` in the SI).

with selectivity for the T_X, T_Y and T_Z sublevels of the triplet state, but results from overpopulation of the high-field $m_s = \pm\frac{1}{2}$ sublevels of the excited quartet state $^4[^3\text{PDI}–^2\text{TEMPO}^\bullet]$. Simulation of the *aea* polarization of the narrow central feature additionally requires the assumption of unequal populations of the nuclear sublevels of the coupled ^{14}N nucleus on TEMPO [31].

4. Electron spin polarization transfer

In addition to ISC, spin-polarized EPR spectra can also arise from electron spin polarization transfer from a spin-polarized precursor state. Examples of processes that involve electron spin polarization transfer are triplet–triplet energy transfer (TTET) and formation of a spin-correlated radical pair (SCRP) from a spin-polarized triplet precursor. These processes typically occur with conservation of spin angular momentum and the polarization patterns therefore reveal information on the nature of the precursor and the relative orientation of the molecular frames of the precursor and detected state.

Triplet–triplet energy transfer occurs via a double electron exchange mechanism and since the operator describing an electrostatic exchange mechanism does not contain spin-dependent terms, the spatial orientation of the spin angular momentum is conserved during the process [77,78]. The populations of the acceptor triplet $p_{\text{A},i}$ in the T_X,T_Y,T_Z basis are therefore determined by the donor populations $p_{\text{D},i}$ as follows

$$p_{\text{A},i} \propto \sum_j \left|\langle T_{\text{A},i}|T_{\text{D},j}\rangle\right|^2 p_{\text{D},j} \qquad i,j = X,Y,Z \tag{13}$$

where $T_{\text{D/A},i}$ are the donor or acceptor triplet states defined in a common coordinate frame. The spin polarization pattern of the acceptor triplet state thus depends on both the populations of the donor triplet and the relative orientation of the ZF interaction frames. The assumption of conservation of spin angular momentum is valid if the transfer results from a purely electrostatic exchange mechanism, and not from magnetic interactions, and if spin–orbit coupling has a negligible effect on the donor and acceptor wavefunctions [79]. Conservation of spin angular momentum during TTET has been demonstrated experimentally for a range of systems [80–82].

In EasySpin, the spin polarization patterns of triplet states formed by TTET can be simulated by calculating the populations $p_{\text{A},X}$, $p_{\text{A},Y}$ and $p_{\text{A},Z}$ of the acceptor based on Eq. 13 and providing them as input to `Sys.initState = {[pAx pAy pAz],'xyz'}`.

This is illustrated in the example of Fig. 8, which shows the spin-polarized EPR spectra of the donor and acceptor triplet states in the light-harvesting complex peridinin-chlorophyll *a*-protein (PCP), where the photoprotection mechanism involves TTET from a chlorophyll triplet state to a lower-lying triplet state of a carotenoid molecule (peridinin) [82]. The EPR spectrum of the donor chlorophyll triplet state exhibits an *eeeaaa* polarization pattern indicative of preferential population of the T_X and T_Y in-plane sublevels by ISC. The *eaeaea* polarization pattern for the peridinin triplet state results from a population distribution obtained by considering the relative orientations between chlorophyll and a unique peridinin molecule based on the crystal structure as well as the orientations of the ZF principal axis systems of the chlorophyll and peridinin triplet states in the respective molecular frames as depicted in Fig. 8 [82].

Similarly to TTET, formation of a spin-correlated radical pair by charge separation from an ISC-polarized triplet state results in equivalent populations of the precursor triplet T_{+1}, T_0 and T_{-1} states and the corresponding radical pair states and therefore a population distribution dependent on the triplet populations p_X, p_Y and p_Z and the orientation of the applied magnetic field [84,12,57].

5. Photoinduced electron transfer processes

Photoinduced electron transfer (PET) processes resulting in the formation of paramagnetic species can also lead to non-Boltzmann population of the spin sublevels and therefore spin-polarized EPR spectra. The fundamental photophysical processes leading to the formation of spin-polarized states in a donor–acceptor system are illustrated in Fig. 9. Photoexcitation leads to an excited singlet state on the donor or acceptor and can be followed by electron transfer forming a radical pair or charge-transfer state $[\text{D}^{\bullet+}\cdots\text{A}^{\bullet-}]$. Since the electron transfer process is spin conserving, the state is formed in a singlet configuration and the spins are correlated. A difference in precession frequency for the spins on the donor and the acceptor, arising from a difference in electron Zeeman interaction or hyperfine interactions, leads to coherent mixing of the singlet and triplet states over time (see inset in Fig. 9). At the

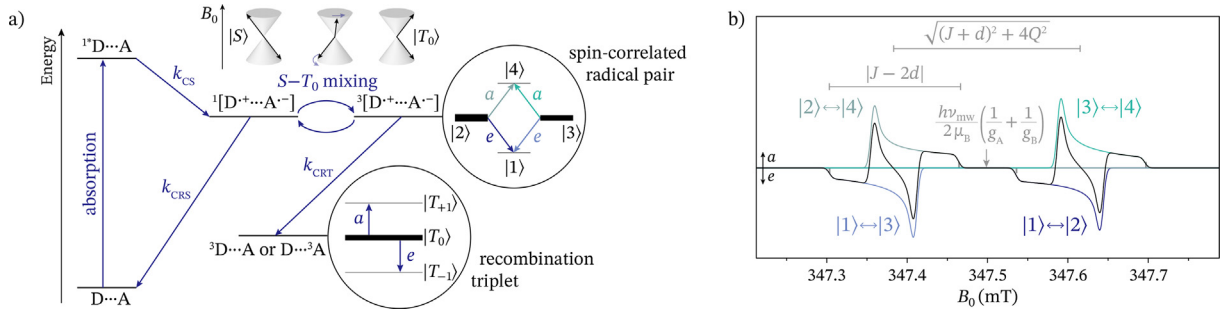

Fig. 9. a) Energy level diagram illustrating the photophysical processes of photoinduced charge separation and charge recombination in donor–acceptor systems. The energy level splitting in the presence of an applied magnetic field and sublevel population resulting from a singlet state precursor are illustrated for the spin-correlated radical pair (or charge transfer) state and the triplet state formed by recombination. b) EPR spectrum for an exchange- and dipolar-coupled SCRP. The contributions from individual transitions between the eigenstates of the systems are shown in color and the overall resulting spectrum is shown in black. (Simulation parameters: $\Delta g = 0.0013$, J = -0.5 MHz, d = 2 MHz).

high magnetic fields typical for EPR, mixing generally occurs only between the $|S\rangle$ and $|T_0\rangle$ states.

The Hamiltonian describing the spin-correlated radical pair state contains electron Zeeman terms for each of the spins as well as an isotropic exchange coupling term and a dipolar electron–electron coupling term

$$\begin{aligned}\hat{\mathscr{H}} &= \tfrac{\mu_B}{h}\boldsymbol{B}_0^T\boldsymbol{g}_A\hat{\boldsymbol{S}}_A + \tfrac{\mu_B}{h}\boldsymbol{B}_0^T\boldsymbol{g}_B\hat{\boldsymbol{S}}_B \\ &\quad + J\hat{\boldsymbol{S}}_A^T\hat{\boldsymbol{S}}_B + \hat{\boldsymbol{S}}_A^T\boldsymbol{D}_{AB}\hat{\boldsymbol{S}}_B\end{aligned} \tag{14}$$

with $\boldsymbol{D}_{AB}$ a matrix with principal elements d, d and $-2d$, where

$$d = \frac{\mu_0}{4\pi h}\frac{g_A g_B \mu_B^2}{r^3}(1 - 3\cos^2\theta) \tag{15}$$

Diagonalization of the Hamiltonian yields the eigenstates

$$\begin{aligned}|4\rangle &= |T_{+1}\rangle \\ |3\rangle &= \cos\phi\,|S\rangle + \sin\phi\,|T_0\rangle \\ |2\rangle &= -\sin\phi\,|S\rangle + \cos\phi\,|T_0\rangle \\ |1\rangle &= |T_{-1}\rangle\end{aligned} \tag{16}$$

where

$$\tan 2\phi = \frac{2Q}{J - \frac{1}{2}d} \qquad Q = \frac{1}{2}\frac{\mu_B}{h}B_0(g_A - g_B) \tag{17}$$

An energy level diagram of the four eigenstates of this system is shown in Fig. 9. The lowest and highest levels, $|1\rangle$ and $|4\rangle$, correspond to the pure triplet states $|T_{-1}\rangle$ and $|T_{+1}\rangle$ and the two intermediate levels have mixed singlet and triplet character, depending on the relative strength of the coupling compared to the difference in the electron Zeeman interaction. Formation of the spin-correlated radical pair from a singlet precursor leads to population of only those states with (partial) singlet character, i.e. states $|2\rangle$ and $|3\rangle$. The resulting spectrum is characterized by two antiphase doublets with a characteristic *eaea* pattern for a singlet-born spin-correlated radical pair with $J < 0$[4] [85,86]. The splitting within each doublet is determined by the dipolar and exchange coupling, while the separation of the two antiphase doublets depends both on the difference in electron Zeeman interaction and the coupling parameters (see Fig. 9b).

The initial density matrix of a singlet-born radical pair, with the diagonal elements corresponding to the sublevel populations, can be calculated as

$$\rho(t=0) = |S\rangle\langle S| \tag{18}$$

which corresponds to the following populations of the two eigenstates with partial singlet character:

$$\begin{aligned}p_2 &= \langle 2\,|\,\rho\,|\,2\rangle = \sin^2\phi \\ p_3 &= \langle 3\,|\,\rho\,|\,3\rangle = \cos^2\phi\end{aligned} \tag{19}$$

Combined with the transition probabilities of the four transitions, this leads to equal intensities of $\frac{1}{2}\sin^2\phi\cos^2\phi$ for all four EPR lines [85]. If the spin-correlated radical pair is instead formed from a triplet state precursor, assuming it is at thermal equilibrium, with almost equal populations of the three triplet sublevels $|T_{-1}\rangle \approx |T_0\rangle \approx |T_{+1}\rangle = \frac{1}{3}$, the resulting sublevel populations are $\frac{1}{3}, \frac{1}{3}cos^2\phi, \frac{1}{3}sin^2\phi$ and $\frac{1}{3}$ and the spectrum is characterized by an opposite *aeae* polarization pattern at one third of the intensity compared to singlet precursor case [55]. If the radical pair initially experiences singlet–triplet mixing, but is no longer interacting at the time of the EPR measurement, the donor and acceptor EPR spectra are oppositely polarized, with the low-field signal emissive and the high-field signal absorptive for a singlet precursor and $J < 0$ [85,86].

Simulation of the EPR spectra of spin-correlated radical pairs allows extraction of information on both the formation mechanism of the radical pair as well as the strength of the interaction between the two components of the pair, which can be translated into structural information. The polarization patterns observed for spin-correlated radical pairs are typically the result of extensive cancellation of strongly overlapping oppositely polarized transitions between the four eigenstates of the system and the EPR spectra are therefore highly sensitive to the dipolar and exchange coupling as well as the relative orientations of the g-frames of donor and acceptor and of the dipolar interaction frame. Extraction of unique and reliable estimates for the large number of fitting parameters typically benefits from global fitting of measurements performed at different frequency bands and prior knowledge of the g-values of donor and acceptor from measurements on the individual radicals. In many cases, more accurate information on the coupling parameters J and d can be obtained by complementing transient EPR with out-of-phase electron spin echo envelope modulation (ESEEM) measurements [87,88].

Spin-polarized EPR spectra of spin-correlated radical pairs can now be simulated in EasySpin by setting up a system of coupled spins with isotropic exchange coupling defined in `Sys.J` and anisotropic dipolar coupling defined in `Sys.dip = [d d -2d]` or with the overall electron–electron coupling defined in `Sys.ee`. The initial state is typically most conveniently defined in the coupled basis,

[4] Note that different conventions exist for the definition of the isotropic exchange Hamiltonian. The definition used here and in EasySpin is $+J\hat{\boldsymbol{S}}_1^T\hat{\boldsymbol{S}}_2$, for which $J < 0$ corresponds to a triplet state that is $|J|$ lower in energy compared to the corresponding singlet state.

T_{+1}, T_0, T_{-1}, S, as `Sys.initState = {[pTp pTO pTm pS],'coupled'}` or using the shortcut `Sys.initState ='singlet'` for a singlet-born radical pair.[5]

The simulation of a spin-polarized state formed after photoinduced electron transfer is illustrated in Fig. 10 on the example of the well-studied first steps of the photosynthetic mechanism in the bacterial reaction center of *Rhodobacter sphaeroides* [90,91]. Photoexcitation of the bacteriochlorophyll dimer P_{865} is followed by a series of electron transfer steps leading to a radical cation on P_{865} and a radical anion on ubiquinone Q_A. Fig. 10 shows the simulated W-band EPR spectra of the individual radical species of the spin-correlated radical pair [90,91]. The complicated spectral shape of the singlet-born spin-correlated radical pair spectrum is a result of the *g*-anisotropies and significant overlap of the spectra of $P_{865}^{\bullet+}$ and $Q_A^{\bullet-}$. Multifrequency EPR studies were essential for the accurate determination of a reliable and unique set of parameters describing the donor–acceptor geometries and interactions in photosynthetic reaction centers by simulation of the spin-correlated radical pair spectrum [92,93].

Also shown in Fig. 10 is the spectrum of the triplet state on the special pair of bacteriochlorophylls P_{865} formed by charge recombination from the radical pair state in a triplet configuration, ${}^3[D^{\bullet+} \cdots A^{\bullet-}]$ [4]. Since recombination occurs with conservation of the polarization of the radical pair state, the spin polarization of the triplet state arises from exclusive population of the triplet $|T_0\rangle$ level in case of recombination from a singlet-born radical pair. Since this triplet formation mechanism selectively populates the high-field triplet sublevels, the resulting polarization pattern *aeeaae* (for $D > 0$) of the triplet spectrum is clearly distinct from any polarization pattern that could be obtained by the ISC mechanism, which is selective for the T_X, T_Y and T_Z states [6].

Simulations of spin-polarized EPR spectra of triplet states formed by radical pair recombination can be performed in EasySpin by specifying the populations of the high-field eigenstates T_{+1}, T_0 and T_{-1} as `Sys.initState = {[pTp pTO pTm],'eigen'}` or using the shortcut `Sys.initState ='TO'`.

Another example of a spin-correlated radical pair from the field of organic photovoltaics is shown in Fig. 11. Photoexcitation of an intermixed blend of the donor polymer poly(3-hexyl-thiophene) (P3HT) and the fullerene derivative [6,6]-phenyl-C_{61}-butyric acid methyl ester (PCBM) as the acceptor leads to a singlet-born spin-correlated radical pair, or charge-transfer, state [94,95,16,54,96]. The differences in the extent of overlap between the spectra of the individual $P3HT^{\bullet+}$ and $PCBM^{\bullet-}$ radicals and in the resolution of the *g*-anisotropy at X- and Q-band result in significantly different spectral shapes of the spin-correlated charge-transfer state. Simulation of spin-correlated charge-transfer states in organic photovoltaic blends in some cases needs to also take into account the intrinsic disorder of the system by including distributions of coupling parameters and of relative orientations of the donor and acceptor molecules or by following previously proposed approaches considering an average over orientations of the dipolar frame or over all possible relative orientations of the *g*-frames of the two polarons [14,54].

The example in Fig. 12 illustrates the case of spin-polarized spin-correlated radical pairs with an initial population of both the *S* and T_0 states for radical pairs in synthetic DNA hairpins designed to control the relative position of a naphthalenediimide (NDI) acceptor and a tetrathiofulvalene (TTF) donor molecule for

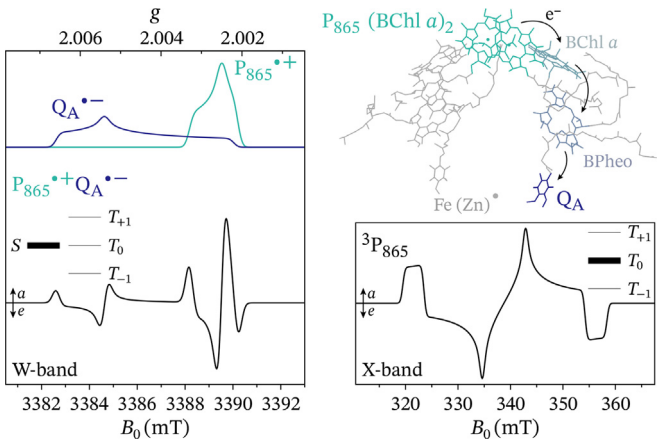

Fig. 10. W-band EPR spectrum of the spin-correlated radical pair generated upon photoexcitation in the bacterial reaction centre of *Rhodobacter sphaeroides* and X-band EPR spectrum of the triplet state formed by recombination. The arrangement of the bacteriochlorophyll dimer P_{865} and the ubiquinone acceptor Q_A in the reaction center is shown on the top right [89]. The SCRP consists of $P_{865}^{\bullet+}$ and $Q_A^{\bullet-}$, the spectra of the individual radicals as well as the dipolar-coupled SCRP state are shown. The simulations were performed for *g*-values of 2.0033, 2.0025 and 2.0021 for $P_{865}^{\bullet+}$ and 2.0066, 2.0054 and 2.0022 for $Q_A^{\bullet-}$, a dipolar coupling of d = 2.32 MHz [90] and relative orientations of the *g*- and dipolar principal axis systems from reference [91] (Ref. [11], orientation II) (see script `PET_SCRP_bRC.m` in the SI). Recombination leads to the formation of a triplet state on the bacteriochlorophyll pair P_{865} and the corresponding spectrum, with a spin polarization resulting from exclusive population of the high-field T_0 triplet sublevel, is shown on the bottom right. The ZF interaction parameters used are D = 546 MHz and E = -105 MHz [4].

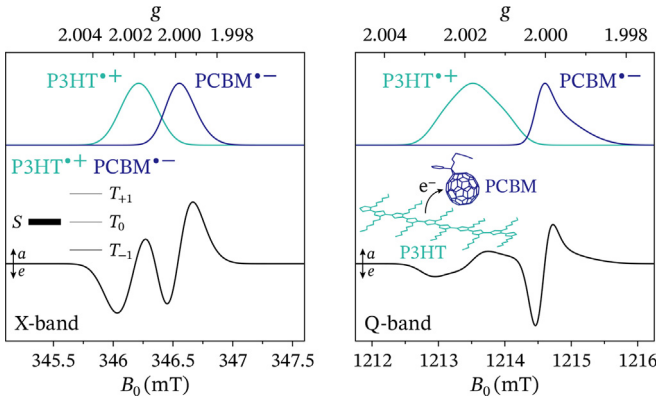

Fig. 11. X- and Q-band EPR spectra of singlet-born spin-correlated radical pairs (polaron pairs) formed upon photoinduced charge separation in blends of P3HT and the fullerene derivative PCBM for organic photovoltaics. The spectra of the individual radicals on the donor and acceptor molecules are shown, as well as the exchange- and dipolar-coupled SCRP spectra. The simulations were performed for *g*-values of 2.0028, 2.0018 and 2.0007 for $P3HT^{\bullet+}$ and 2.0001, 2.0001 and 1.9989 for $PCBM^{\bullet-}$, an exchange coupling of J = -3 MHz and a dipolar coupling of d = -1 MHz [54] (see script `PET_SCRP_P3HTPCBM.m` in the SI).

applications in quantum information science [97]. The EPR spectra for an exchange- and dipolar-coupled radical pair separated by four DNA basepairs and for a more weakly dipolar-coupled radical pair separated by six basepairs are simulated considering contributions of an initial T_0 population of 0.19 and 0.27, respectively, attributed to singlet–triplet mixing already in the intermediate $NDI^{\bullet-}$–$purine^{\bullet+}$ radical pairs.

[5] In some cases, it might be useful to simulate contributions from the four individual transitions separately in EasySpin. However, care must be taken in the interpretation of this output for spin systems where the energy level ordering changes with orientation, as the assignment of contributions for individual orientations of the magnetic field to the overall summed spectra for each transitions in EasySpin relies on an ordering of states by increasing energy.

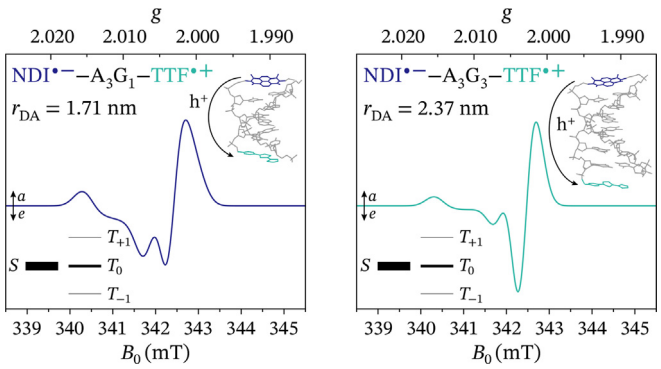

Fig. 12. X-band EPR spectra of spin-correlated radical pairs formed after photoinduced hole transfer in synthetic DNA hairpins of different lengths modified with an NDI acceptor and a TTF donor. The simulations were performed for *g*-values of 2.0076, 2.0154 and 2.0021 for $TTF^{\bullet+}$ and 2.0046, 2.0047 and 2.0022 for $NDI^{\bullet-}$, and with an exchange coupling of J = -2.6 MHz and a dipolar coupling of d = 10.4 MHz (r = 1.71nm) for NDI-A_3G_1-TTF and J = 0 MHz and a dipolar coupling of d = 3.9 MHz (r = 2.37nm) for NDI-A_3G_3-TTF and included fractional contributions of an initial T_0 population of 0.19 and 0.27, respectively [97] (see script `PET_SCRP_TTFNDI.m` in the SI).

6. Singlet Fission

Spin-polarized EPR spectra can also result from singlet fission (SF), a spin-allowed process involving two organic molecules that converts a photogenerated singlet exciton into two lower-energy triplet excitons in systems satisfying the energy requirement $E(S_1) \geqslant 2E(T_1)$ [98]. Spin angular momentum conservation dictates that singlet fission occurs through a spin-correlated triplet pair in an initial singlet state, $^1(T_1T_1)$ (Fig. 13). If the lifetime of the $^1(T_1T_1)$ state is sufficiently long, spin mixing between the singlet $^1(T_1T_1)$ and the quintet $^5(T_1T_1)$ states can occur, driven by fine-structure interactions and resulting in a spin-polarized EPR spectrum of the coupled triplet pair [18,19,99]. Further evolution of the triplet pair state through decoherence, triplet exciton diffusion, or triplet–triplet annihilation can result in uncorrelated triplet states (Fig. 13). Since the spin-correlated triplet pair is initially formed in a singlet state, the spin polarization of the observed EPR spectra is typically determined by selective population of the $m_S = 0$ sublevel for the coupled triplet pair as well as for the resulting uncorrelated triplet states (see Fig. 13). While the initial and final states of singlet fission are well understood, the intervening dynamics are quite complex and still a very active area of research [100–103].

The spin Hamiltonian describing a pair of coupled triplet states, A and B, is given by:

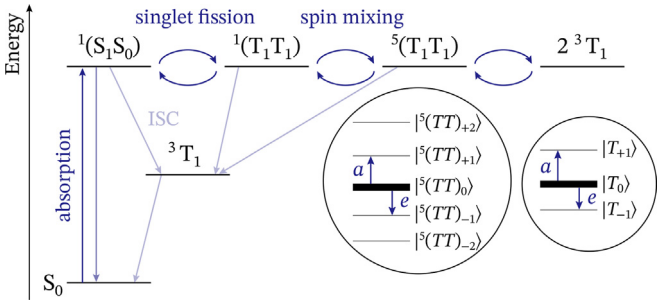

Fig. 13. Energy level diagram illustrating the photophysical processes in systems allowing singlet fission and illustration of the sublevel populations for coupled triplet pairs and individual triplet states.

$$\hat{\mathscr{H}} = \begin{aligned} &\tfrac{\mu_B}{h}\boldsymbol{B}_0^T\boldsymbol{g}_A\hat{\boldsymbol{S}}_A + \hat{\boldsymbol{S}}_A^T\boldsymbol{D}_A\hat{\boldsymbol{S}}_A \\ &+\tfrac{\mu_B}{h}\boldsymbol{B}_0^T\boldsymbol{g}_B\hat{\boldsymbol{S}}_B + \hat{\boldsymbol{S}}_B^T\boldsymbol{D}_B\hat{\boldsymbol{S}}_B \\ &+\hat{\boldsymbol{S}}_A^T\boldsymbol{D}_{AB}\hat{\boldsymbol{S}}_B + J_{AB}\hat{\boldsymbol{S}}_A^T\hat{\boldsymbol{S}}_B \end{aligned} \tag{20}$$

including the electron Zeeman and zero-field interactions for each triplet state along with the exchange, J_{AB}, and dipole–dipole, $\boldsymbol{D}_{AB}$, coupling terms between the two triplets. In the coupled basis, the nine states of this spin Hamiltonian consist of one singlet, $^1(TT)$, three triplet, $^3(TT)$, and five quintet, $^5(TT)$, states [104,105]. The spin wavefunctions of the $^1(TT)$ and $^5(TT)$ states are symmetric with respect to triplet exchange, allowing mixing of these states, while the $^3(TT)$ state is anti–symmetric and does not mix, with the exception of avoided-crossing points [105,101].

Spin-polarized EPR spectra of coupled triplet pairs and uncoupled triplet states formed in singlet fission processes can be simulated in EasySpin by defining the interaction parameters describing the spin system and included in Eq. 20, and specifying the sublevel population distribution in `Sys.initState` using the eigenbasis of the spin Hamiltonian or the coupled basis, as illustrated in the following examples. The coupled triplet pair can be described either in terms of a quintet state (for collinear triplets in the strong exchange limit) or explicitly as a pair of exchange- and dipolar-coupled triplet states. While the use of the full triplet pair spin Hamiltonian allows for a more accurate spectral simulation, extraction of unique and reliable values for the large number of required fitting parameters typically requires information from additional measurements. The triplet *g*-value and ZF parameters can often be obtained through fitting of the isolated triplet, and the relative orientations of the triplet pair can be estimated from experimental or modeled structural information. In the strong-coupling regime, the spectrum is relatively insensitive to the exchange interaction J_{AB}, so generally only a lower limit can in some cases be determined by measurements performed at different frequencies; a more accurate determination of the exchange coupling is possible through field-dependent fluorescence or photoluminescence measurements [106,107,101]. The spin polarization is typically best defined through the energy-ordered populations of the high-field eigenstates using `Sys.initState = {[pS pTm pT0 pTp pQm2 pQm1 pQ0 pQp1 pQp2],'eigen'}` (for $J_{AB} > 0$). In the strong-coupling regime, only the $^5(TT)_0$ sublevel is initially populated (`pQ0 = 1`), but when J_{AB} is no longer large relative to the other terms in the spin Hamiltonian, population of the $^5(TT)_{-2}$ and $^5(TT)_{-1}$ sublevels can also occur [99,100,102]. Definition of the initial state as a density matrix in the coupled or uncoupled basis is recommended in the weak- to moderate-coupling regime, since the energy-ordered eigenstates of the system may change spin character as a function of orientation when J_{AB} is on the same order of magnitude or smaller than the other terms in the spin Hamiltonian.

The presence of spectral features from both coupled triplet pairs as well as uncorrelated triplet states in most systems involved in singlet fission can in some cases necessitate additional nutation experiments for an unequivocal assignment of the different observed spectra and transitions [18,19,99,100].

The different approaches in simulating spin-polarized EPR spectra of triplet pairs formed by singlet fission are illustrated in Fig. 14 on the example of TIPS-tetracene and TIPS-pentacene. Fig. 14a shows the EPR spectrum of TIPS-tetracene thin films, which, at low temperatures, contains contributions from both coupled triplet pairs as well as uncoupled or weakly coupled tetracene triplets [18]. The ratio of $\frac{1}{3}$ between the D parameter of the two spectral contributions indicates that the system is in the strong-exchange coupling regime ($J_{AB} \gg \frac{\mu_B}{h} g\boldsymbol{B}_0$) and suggests collinear ZF interaction frames for the two triplet states. The spectrum can therefore be

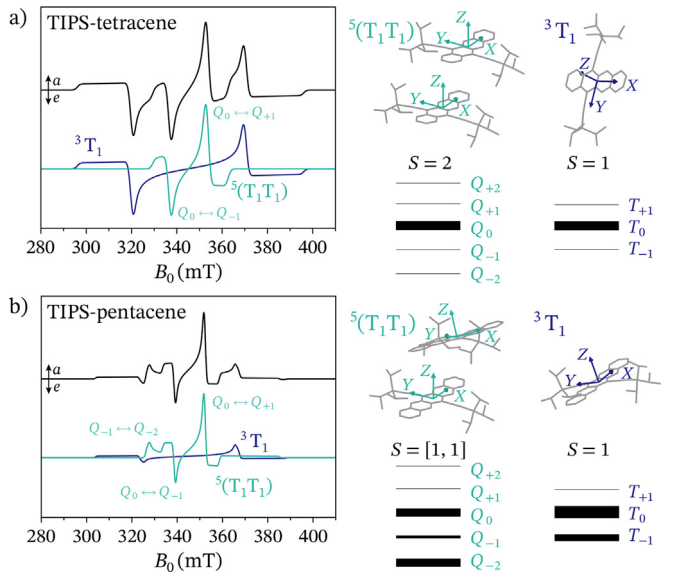

Fig. 14. a) EPR spectrum of non-interacting triplets (blue) and pairs of strongly coupled triplets (green) in TIPS-tetracene thin films. The overall spectrum is a sum of both contributions. The simulations were performed for a ZF D parameter of 1401 MHz for the non-interacting triplet state and $\frac{1}{3}D$ for the coupled triplet pair forming a quintet state [18]. In both cases only the $m_S = 0$ sublevel is populated (see script `SF_quintet_TIPStetracene.m` in the SI). b) EPR spectrum of non-interacting triplets (blue) and pairs of coupled triplets (green) in TIPS-pentacene films. The overall spectrum is a sum of both contributions. The simulations were performed for a g-value of 2.002 and ZF parameters D = 1180 MHz and E = -18 MHz for each triplet state, and an exchange coupling of J = 30 GHz and a dipolar coupling of d = 10 MHz for the coupled triplet pair [100]. The relative orientation of the principal axes of the ZF interaction is defined by Euler angles of $\alpha = 120°$ and $\beta = 20°$. The population distributions for the single triplet and for the coupled pair of triplets were $p_{-2} : p_{-1} : p_0 : p_{+1} : p_{+2} = 0.43 : 0.13 : 0.44 : 0 : 0$ and $p_{-1} : p_0 : p_{+1} = 0.35 : 0.65 : 0$, respectively [100] (see script `SF_tripletpair_TIPSpentacene.m` in the SI).

simulated as a pure $S = 2$ quintet state with a zero–field interaction of $\frac{1}{6}(D_A + D_B)$. The selective population of the $^5(TT)_0$ sublevel results in the characteristic *aeeaae* polarization pattern [18], which can be simulated by specifying the populations in the eigenbasis of the spin Hamiltonian as `Sys.initState = {[0 0 1 0 0],'eigen'}`.

The uncorrelated triplet states formed from the coupled triplet pairs inherit the polarization of the parent (T_1T_1) state and are therefore also selectively populated in the T_0 sublevel. The corresponding spectrum exhibits the *aeeaae* polarization previously also observed for triplet states formed by recombination from singlet-born radical pairs and can be simulated analogously.

Fig. 14b shows the EPR spectrum observed for disordered aggregates of TIPS-pentacene. The differences both in the spin polarization pattern as well as the ratio of the peak separations of the triplet pair and triplet contributions between this spectrum and that of TIPS-tetracene discussed above, indicate that this system needs to be treated explicitly as a pair of coupled triplet states [100]. The spectrum of the coupled triplet pair is simulated based on the ZF parameters of the individual triplet and a relative orientation of the ZF interaction frames shifted slightly from collinearity. The asymmetry in the central part of the spectrum and an additional absorptive feature not assignable to the transitions between the $^5(TT)_0$ and $^5(TT)_{\pm1}$ states at low fields result from a distribution of populations between the $^5(TT)_0$, $^5(TT)_{-1}$ and $^5(TT)_{-2}$ states attributed to multiexciton diffusion from an ordered stacked pair to a more disordered trap state resulting in SQ_0, SQ_{-1}, and SQ_{-2} mixing [100]. The uncorrelated triplet states formed again inherit the spin polarization from their triplet pair precursor,

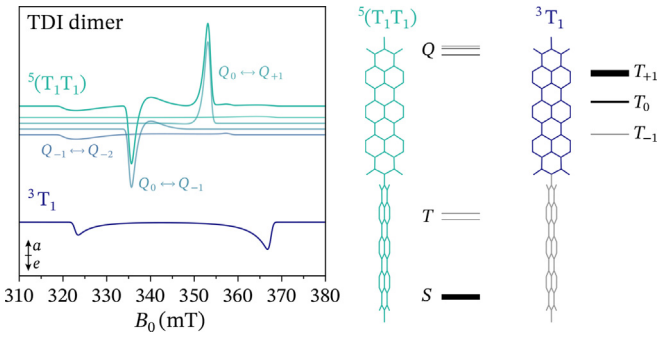

Fig. 15. EPR spectra of spin-polarized states formed as a result of singlet fission for a terrylenediimide dimer in a nematic liquid crystal [101]. The spectrum of the coupled pair of triplets is shown on top, with the individual transitions contributing to the overall spectrum, and the spectrum of an isolated triplet state is shown on the bottom. The simulations were performed for a g-value of 2.00237 and ZF parameters D = 861 MHz and E = -131 MHz for each TDI triplet state. For the coupled pair of triplets, an exchange coupling of J = 8.13 GHz and a dipolar coupling of d = 12 MHz was used. The relative orientation of the principal axes of the ZF interaction matches the perpendicular arrangement of the two TDI units. For the coupled pair of triplets, states with a singlet component are initially populated, for the individual uncoupled triplet state populations of $p_{-1} : p_0 : p_{+1} = 0 : 0.24 : 0.76$ were used [101]. The preferential orientation of the molecule with respect to the magnetic field was modeled using `Exp.Ordering = +5` (see script `SF_triplet-pair_TDI2.m` in the SI and section on partially ordered systems for details).

resulting in the observed *aeeaae* spin polarization with different intensities of the $T_{-1} \leftrightarrow T_0$ and $T_0 \leftrightarrow T_{+1}$ transitions.

The example in Fig. 15 shows the EPR spectra for a covalently linked terrylenediimide (TDI) dimer undergoing singlet fission [101]. This dimer was aligned in a nematic liquid crystal in order to obtain a near-single-crystal-like resolution of the transitions. The perpendicular arrangement of the conjugated π-systems of the two terrylenediimide units results in a relatively weak exchange coupling between the two triplet states formed by singlet fission. The spin polarization of the three principal transitions of the (T_1T_1) state contributing to the spectrum was simulated by modeling the system as a coupled pair of triplet states and calculating the sublevel populations from the overlap between the pure singlet state and the eigenstates of the spin Hamiltonian using the shortcut `Sys.initState ='singlet'`. This approach is required to account for mixing between the $^3(TT)_{+1}$ and $^5(TT)_{-1}$ states at an avoided crossing, producing a state with significant singlet character and resulting in the additional emissive transition at low fields [101]. A further consequence of this mixing is an increased probability of triplet–triplet annihilation, yielding a single triplet state with significant population in the T_{+1} triplet sublevel due to conservation of spin angular momentum in addition to the expected T_0 sublevel and resulting in a fully emissive triplet state spectrum [101].

7. Photoselection

The lineshape of EPR spectra recorded using photoexcitation with polarized light is typically affected by photoselection: the photoexcitation probability for a specific molecular orientation depends on the relative orientation of the electric-field vector of the incident radiation and the optical transition dipole moment (TDM) of the molecule; therefore molecules with different orientations with respect to the transition dipole moment contribute with different intensity to the EPR spectrum [108,109].

The excitation probability for a molecule with a specific orientation in the laboratory frame is defined as

$$p(\phi, \theta, \chi) = \left(\boldsymbol{\mu}_{\mathrm{opt,L}}^{\mathrm{T}} \boldsymbol{E}\right)^2 \tag{21}$$

where $\boldsymbol{\mu}_{\mathrm{opt,L}}$ specifies the orientation of the optical transition dipole moment vector in the laboratory frame, $\boldsymbol{E}$ is the electric-field vector of the incident light and the angles ϕ, θ and χ relate the laboratory and molecular frames (Fig. 16a). The integration over χ can be solved analytically, giving

$$p(\phi,\theta) = \int (\boldsymbol{\mu}_{opt,L}^{T}\boldsymbol{E})^2 d\chi = \tfrac{1}{2}(\mu_{\mathrm{opt,Lx}}^2 + \mu_{\mathrm{opt,Ly}}^2)(E_x^2 + E_y^2) + \mu_{\mathrm{opt,Lz}}^2 E_z^2 \quad (22)$$

The calculation of photoselection probabilities based on this equation is now implemented in EasySpin within the `photoselect` function.

The simulation of photoselection effects on the EPR spectra of photoexcited states requires the orientation of the optical transition dipole moment in the molecular frame to be specified within the spin system structure as `Sys.TDM`. EasySpin allows the definition of arbitrary photoexcitation and polarization geometries in terms of the propagation direction of the excitation light beam, $\boldsymbol{k}$, in the laboratory frame and the polarization angle α defining the direction of the electric field vector $\boldsymbol{E}$ in the plane perpendicular to the propagation direction (see Fig. 16a) in the experimental parameter structure as `Exp.lightBeam = {k alpha}`. The most common photoexcitation geometry with the propagation direction of the light beam aligned with the $\boldsymbol{y}_{\mathrm{L}}$ axis of the laboratory frame is depicted in Fig. 16b, and photoexcitation with the electric field vector parallel or perpendicular to the external magnetic field $\boldsymbol{B}_0$ can easily be specified using the keywords `'parallel'` and `'perpendicular'` in `Exp.lightBeam`.

Photoselection effects can be reduced with the use of a depolarizer, however residual effects remain since the electric-field vector is always perpendicular to the direction of light propagation [110]. The EPR spectra of states photoexcited with unpolarized light can differ quite significantly from the spectrum expected for isotropic excitation, which can be reconstructed as the sum of one $\boldsymbol{E}_{\mathrm{light}} \| \boldsymbol{B}_0$ spectrum and two $\boldsymbol{E}_{\mathrm{light}} \perp \boldsymbol{B}_0$ spectra. Simulation of photoselection effects resulting from excitation with an unpolarized light beam is implemented in EasySpin based on the orientation-dependent photoexcitation probability defined as

$$p_{\mathrm{unpol}}(\phi,\theta) = \tfrac{1}{2}(1 - p_{\boldsymbol{k}}(\phi,\theta))$$
$$p_{\boldsymbol{k}}(\phi,\theta) = \tfrac{1}{2}(\mu_{\mathrm{opt,Lx}}^2 + \mu_{\mathrm{opt,Ly}}^2)(k_x^2 + k_y^2) + \mu_{\mathrm{opt,Lz}}^2 k_z^2 \quad (23)$$

Photoselection with unpolarized light can be simulated by specifying `Exp.lightBeam ='unpolarized'` for the default propagation direction along $\boldsymbol{y}_{\mathrm{L}}$ or by setting α to `NaN` for arbitrary propagation directions.

Simulations including a contribution with isotropic excitation (i.e. an electric-field vector distributed uniformly in all directions) to account for scattering or energy transfer effects can be performed by specifying the fraction of the isotropic contribution in `Exp.lightScatter`.

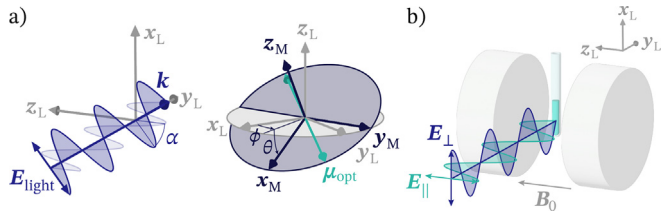

Fig. 16. a) Illustration of the parameters defining an arbitrary photoexcitation geometry: the propagation direction $\boldsymbol{k}$ and the polarization angle α, specifying the orientation of the electric field vector $\boldsymbol{E}$ in the laboratory frame. The orientation of the optical transition dipole moment $\boldsymbol{\mu}_{\mathrm{opt}}$ is defined with respect to the molecular frame, which is related to the laboratory frame through rotation by Euler angles ϕ, θ and χ (= 0). b) Schematic illustration of the typical photoexcitation geometry with light propagation along the $\boldsymbol{y}_{\mathrm{L}}$ axis of the laboratory frame and $\boldsymbol{E}_{\mathrm{light}}$ parallel or perpendicular to $\boldsymbol{B}_0$.

The effect of photoexcitation with linearly polarized light on the EPR spectral shapes of photoexcited triplet states is illustrated in Fig. 17 on the example of an asymmetric acceptor-substituted zinc porphyrin [111]. The EPR spectra corresponding to photoexcitation with light polarized parallel and perpendicular to the external magnetic field are compared for two different excitation wavelengths corresponding to two perpendicular optical transition moments lying in the plane of the molecule, Q_x and Q_y. Due to a near-perfect alignment of the zero-field Y axis with Q_y, photoexcitation with light polarized parallel to the magnetic field at wavelengths corresponding to this transition (544 nm) preferentially excites molecules with the zero-field Y axis aligned with the static magnetic field, while light with perpendicular polarization excites molecules with their zero-field X and Z axes aligned with the field. Similarly, the spectra for photoexcitation at wavelengths corresponding to the Q_x transition (592 nm) show enhancement of the contributions from the X transition for light polarized parallel to B_0, and of the Y and Z transitions for light polarized perpendicular to B_0. The simulations take into account contributions from isotropic excitation as well as contributions from both optical transitions, due to slight overlap of the absorption bands, as described in reference [111].

Knowledge of the orientation of the optical transition dipole moments with respect to the molecular structure in molecules such as these has been exploited for the determination of the orientation of the ZF interaction frame of the molecule. This is particularly useful since the orientation of the axis of maximum dipolar coupling, Z, in the molecular frame has implications for the sign of the corresponding zero-field interaction parameter D, i.e. assignment of the ZF Z axis to the out-of-plane axis corresponds to $D > 0$ in porphyrin and chlorophyll molecules [108,112,69,111]. Similarly, if the orientation of the principal axes of the ZF interaction matrix with respect to the molecular frame is known, EPR experiments with photoselection can provide information on the orientation of the optical transition dipole moment, as recently demonstrated for excitonically coupled chlorophylls [113].

8. Partially ordered systems

In solid-state samples or samples prepared in liquid–crystal solvents, additional orientational effects can arise due to a non-

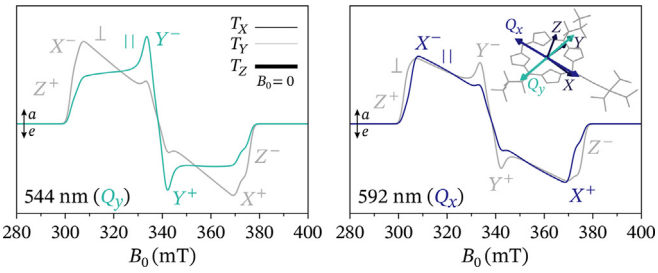

Fig. 17. EPR spectra of the photoexcited triplet states of a substituted zinc porphyrin photoexcited at wavelengths corresponding to the porphyrin Q_x and Q_y optical transitions for light polarized parallel (∥) and perpendicular (⊥) to the static magnetic field [111]. The orientations of the optical transition dipole moments and of the ZF interaction frame are depicted with respect to the molecule in the inset. The spectra were simulated with D = 1033 MHz, E = -272 MHz, $p_X : p_Y : p_Z = 0.10 : 0 : 0.90$, resulting from ISC, and an orientation of the optical transition dipole moment Q_x (ca. 592 nm) at θ = 74°, ϕ = -3°, and Q_y (ca. 544 nm) at θ = 74°, ϕ = 87° with respect to the ZF interaction frame (see script `Photoselection_triplet_ZnP.m` in the SI). The simulations for each excitation wavelength contain contributions from isotropically excited triplet states and from the other transition dipole moment (see SI of reference [111] for details)..

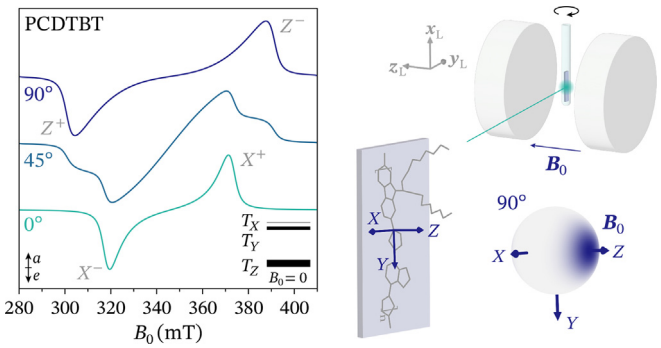

Fig. 18. EPR spectra of the photoexcited triplet state of PCDTBT in films drop-cast onto a substrate for different orientations with respect to the magnetic field (90° corresponding to the out-of-plane direction of the substrate aligned with the magnetic field). The PCDTBT polymer assumes a face-on alignment in the film with the ZF Z axis lying within a cone of 52° from the out-of-plane direction. The spectra were simulated with D = 1268 MHz, E = -101 MHz, $p_X : p_Y : p_Z = 0 : 0.31 : 0.69$ resulting from ISC [114] (see script `PartialOrder_triplet_PCDTBT.m` in the SI).

random distribution of molecular orientations. The spectral shape of EPR spectra then depends on the orientation of the sample with respect to the static magnetic field and on the degree of ordering. EasySpin includes simulation capabilities for systems exhibiting partial order through definition of an orientational distribution function and the orientation of the sample in the spectrometer, which can be used for spin-polarized systems as well.

Simulation of partial ordering effects requires the definition of an orientational distribution function in `Exp.Ordering`, representing the probability of different molecular frame orientations with respect to a sample-fixed frame. The orientational distribution can be provided through an arbitrary function of the angles θ and ϕ, or by specifying λ, which is used to calculate the orientational distribution as a function of the angle θ based on the equation:

$$P(\theta) = \exp(-\frac{1}{2}\lambda(3\cos^2\theta - 1)) \quad (24)$$

Simulation of the rotation of a partially ordered sample in the external magnetic field is implemented in EasySpin through the field `Exp.SampleRotation`, where a rotation angle and rotation axis can be defined, with the $\boldsymbol{x}_L$ laboratory frame as the default axis for sample rotation (see Fig. 18). This reorients the orientational distribution with respect to the laboratory frame.

The simulation of experimentally observed partial ordering effects can provide information on the degree of ordering and the orientation of molecules in a film on a substrate or in a liquid crystal. Fig. 18 illustrates the variation of the spectral shape of the photoexcited triplet state in a film of the organic semiconducting polymer PCDTBT with substrate orientation [114]. The observation of contributions mainly from the Z transitions for films oriented with the out-of-plane axis aligned with the magnetic field (90°) is indicative of a relatively strong face-on alignment of the polymer on the substrate.

9. Spin-selective dynamics

The discussion so far has focused on the simulation of EPR spectra recorded at short times after photoexcitation, with spin polarizations directly determined by the formation mechanism. In many cases, the observed spin polarization changes over time as a consequence of dynamical and relaxation processes. The same approach to simulation of spin-polarized EPR spectra can easily be extended to model a time dependence determined by spin-selective dynamics. The time dependence of spin sublevel populations can be modeled by setting up and solving a system of differential equations. The spectrum can then be simulated at selected time points by specifying the sublevel populations corresponding to that time point in `Sys.initState`. The full two-dimensional time-resolved EPR data can be obtained using an external loop and calling `pepper` for each of the required time points.

This approach can be used, for example, to model the evolution of the spin polarization of a photoexcited triplet state as shown in Fig. 19. In a triplet state formed by ISC, both the population and decay rate constants are selective for the T_X, T_Y and T_Z states and are determined by matrix elements of the spin–orbit coupling Hamiltonian, however considering the singlet excited state S_1 for population and the singlet ground state S_0 for decay [116]. If the relative sublevel population and decay rates differ significantly, the polarization pattern of the triplet state spectrum can change considerably over time. The example in Fig. 19 shows the evolution of the spin polarization of the triplet state of peridinin in peridinin-chlorophyll *a*-protein [115]. The triplet state is formed by triplet–triplet energy transfer and has an initial *eaeaea* polarization due to population of mainly the T_Z and T_Y sublevels. The triplet state then preferentially decays through the T_X and T_Z levels leading to the polarization pattern evolving to *aaeaee* before decaying completely.

The current simulation capabilities for spin-polarized systems in EasySpin cover any dynamical effects that can be modeled as a set of kinetic equations describing the time-dependence of spin-sublevel populations. The inclusion of coherence effects such as the so-called quantum beats observed for photosynthetic radical pairs, transient nutations arising from the precession of the magnetization about the microwave B_1 field in transient EPR (Torrey oscillations), a rigorous inclusion of relaxation and diffusive dynamics, require more advanced simulation approaches based on the Liouville–von Neumann or the stochastic Liouville equation [117,118,45], that are currently not implemented in EasySpin.

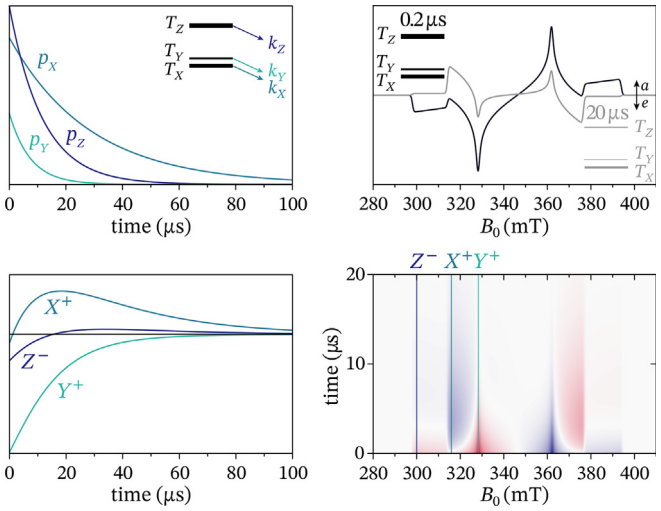

Fig. 19. Time evolution of the spin polarization of the excited triplet state of a peridinin molecule formed by TTET in the peridinin-chlorophyll *a*-protein modeled by considering sublevel-specific decay rate constants k_x, k_y and k_z. The time dependence of the triplet sublevel populations, transients at the low-field canonical positions, spectra at different times after photoexcitation as well as the full simulated time-dependence of the spin-polarized EPR spectrum (red = emissive, blue = absorptive) are shown. The ZF interaction parameters used in the simulation are D = -1345 MHz and E = 134 MHz, the initial relative sublevel populations are $p_X : p_Y : p_Z = 0.37 : 0.18 : 0.45$ and the decay constants (in μs^{-1}) $k_X : k_Y : k_Z = 0.035 : 0.135 : 0.085$ [115] (see script `Dynamics_triplet_PCP.m` in the SI).

10. Conclusions

The spin polarization exhibited by EPR spectra of paramagnetic species created by photoexcitation can provide a wealth of information on photophysical and photochemical processes relevant to a wide range of research fields and applications. As illustrated in the provided examples, spin-polarized species play a significant role in a variety of biological processes and in molecules and materials for optoelectronics, molecular electronics, and quantum information science.

The ability to extract information on the molecular and electronic structure of spin-polarized systems as well as their dynamics of formation relies heavily on simulation of experimental transient EPR spectra. The inclusion of support for the simulation of spin polarization arising from a variety of different mechanisms and for different spin systems in the EPR simulation toolbox EasySpin facilitates the analysis of EPR spectra of spin-polarized systems. The integration with EasySpin additionally provides easy access to many EPR data analysis routines, in particular the extensive support for least-squares fitting.

The availability of a general and user-friendly simulation framework including support for spin-polarized systems improves comparability and makes this field more easily accessible to the wider research community beyond groups with extensive EPR expertise. This is particularly valuable given the increasingly important role of spin polarization and spin-polarized species in new application areas such as organic electronics, with spin-correlated radical pairs, triplet states and triplet pairs playing a role in OLEDs and organic solar cells, biological structure determination, with spin-polarized triplet states used as spin labels to increase sensitivity in dipolar EPR, and quantum information science, where photoexcited spin-polarized states are being explored as molecular qubits [119].

Funding

This work was partially funded by the National Science Foundation (CHE-2154302, S.S.). C.E.T. is thankful to the Royal Society for a University Research Fellowship (URF\R1\201071) and to Balliol College, Oxford for an Early Career Fellowship. The work by M.D. K. was supported as part of the Center for Molecular Quantum Transduction (CMQT), an Energy Frontier Research Center funded by the U.S. Department of Energy, Office of Science, Basic Energy Sciences, under Award DE-SC0021314.

Data availability

The Matlab code files are attached in the supporting information.

Declaration of Competing Interest

The authors declare that they have no known competing financial interests or personal relationships that could have appeared to influence the work reported in this paper.

Appendix A. Supplementary material

Supplementary data associated with this article can be found, in the online version, at https://doi.org/10.1016/j.jmr.2023.107410.

References

[1] H. Levanon, S.I. Weissman, Spin polarization in the photoexcitation of the triplet state of phenazine in a rigid glass, Isr. J. Chem. 10 (1972) 1–5, https://doi.org/10.1002/ijch.197200002.
[2] R.H. Clarke, Magnetic resonance studies of optical spin polarization in triplet state anthracene, Chem. Phys. Lett. 6 (5) (1970) 413–416, https://doi.org/10.1016/0009-2614(70)85179-X.
[3] K.A. McLauchlan, D.G. Stevens, Flash photolysis electron spin resonance, Acc. Chem. Res. 21 (1988) 54–59, https://doi.org/10.1021/ar00146a002.
[4] M.C. Thurnauer, J.J. Katz, J.R. Norris, The triplet state in bacterial photosynthesis: Possible mechanisms of the primary photo-act, Proc. Natl. Acad. Sci. 72 (9) (1975) 3270–3274, https://doi.org/10.1073/pnas.72.9.3270.
[5] H. Levanon, J.R. Norris, The photoexcited triplet state and photosynthesis, Chem. Rev. 78 (3) (1978) 185–198, https://doi.org/10.1021/cr60313a001.
[6] D.E. Budil, M.C. Thurnauer, The chlorophyll triplet state as a probe of structure and function in photosynthesis, Biochim. Biophys. Acta 1057 (1) (1991) 1–41, https://doi.org/10.1016/S0005-2728(05)80081-7.
[7] P.J. Hore, D.J. Riley, J.J. Semlyen, G. Zwanenburg, A.J. Hoff, Analysis of anisotropic electron spin polarization in the photosynthetic bacterium Rhodospirillum rubrum. Evidence that the sign of the exchange interaction in the primary radical pair is positive, Biochim. Biophys. Acta 1141 (1993) 221–230, https://doi.org/10.1016/0005-2728(93)90046-I.
[8] K. Hasharoni, H. Levanon, S.R. Greenfield, D.J. Gosztola, W.A. Svec, M.R. Wasielewski, Radical pair and triplet state dynamics of a photosynthetic reaction-center model embedded in isotropic media and liquid crystals, J. Am. Chem. Soc. 118 (42) (1996) 10228–10235, https://doi.org/10.1021/ja961919e.
[9] D. Carbonera, M. Di Valentin, G. Agostini, G. Giacometti, P.A. Liddell, D. Gust, A.L. Moore, T.A. Moore, Energy transfer and spin polarization of the carotenoid triplet state in synthetic carotenoporphyrin dyads and in natural antenna complexes, Appl. Magn. Reson. 13 (3–4) (1997) 487–504, https://doi.org/10.1007/BF03162222.
[10] W. Lubitz, F. Lendzian, R. Bittl, Radicals, radical pairs and triplet states in photosynthesis, Acc. Chem. Res. 35 (5) (2002) 313–320, https://doi.org/10.1021/ar000084g.
[11] A. van der Est, P.K. Poddutoori, Time-Resolved EPR in Artificial Photosynthesis, in: H.J. Hou, M.M. Najafpour, G.F. Moore, S.I. Allakhverdiev (Eds.), Photosynthesis: Structures, mechanisms, and applications, Ch. 18, Springer, Cham, 2017, pp. 359–387, https://doi.org/10.1007/978-3-319-48873-8.
[12] S. Weber, T. Biskup, A. Okafuji, A.R. Marino, T. Berthold, G. Link, K. Hitomi, E.D. Getzoff, E. Schleicher, J.R. Norris, Origin of light-induced spin-correlated radical pairs in cryptochrome, J. Phys. Chem. B 114 (45) (2010) 14745–14754, https://doi.org/10.1021/jp103401u.
[13] J. Xu, L.E. Jarocha, T. Zollitsch, M. Konowalczyk, K.B. Henbest, S. Richert, M.J. Golesworthy, J. Schmidt, V. Déjean, D.J.C. Sowood, M. Bassetto, J. Luo, J.R. Walton, J. Fleming, Y. Wei, T.L. Pitcher, G. Moise, M. Herrmann, H. Yin, H. Wu, R. Bartölke, S.J. Käsehagen, S. Horst, G. Dautaj, P.D.F. Murton, A.S. Gehrckens, Y. Chelliah, J.S. Takahashi, K.-W. Koch, S. Weber, I.A. Solov, C. Xie, S.R. Mackenzie, C.R. Timmel, H. Mouritsen, P.J. Hore, Magnetic sensitivity of cryptochrome 4 from a migratory songbird, Nature 594 (2021) 535–540, https://doi.org/10.1038/s41586-021-03618-9.
[14] L. Pasimeni, M. Ruzzi, M. Prato, T. Da Ros, G. Barbarella, M. Zambianchi, Spin-correlated radical ion pairs generated by photoinduced electron transfer in composites of sexithiophene/fullerene derivatives: a transient EPR study, Chem. Phys. 263 (2001) 83–94, https://doi.org/10.1016/S0301-0104(00)00339-6.
[15] F. Kraffert, R. Steyrleuthner, S. Albrecht, D. Neher, M.C. Scharber, R. Bittl, J. Behrends, Charge separation in PCPDTBT:PCBM blends from an EPR perspective, J. Phys. Chem. C 118 (2014) 28482–28493, https://doi.org/10.1021/jp509650v.
[16] J. Niklas, S. Beaupré, M. Leclerc, T. Xu, L. Yu, A. Sperlich, V. Dyakonov, O.G. Poluektov, Photoinduced dynamics of charge separation: from photosynthesis to polymer–fullerene bulk heterojunctions, J. Phys. Chem. B 119 (2015) 7407–7416, https://doi.org/10.1021/jp511021v.
[17] J. Niklas, O.G. Poluektov, Charge Transfer Processes in OPV Materials as Revealed by EPR Spectroscopy, Adv. Energy Mater. 7 (10) (2017) 1602226-1–1602226-28, https://doi.org/10.1002/aenm.201602226.
[18] L.R. Weiss, S.L. Bayliss, F. Kraffert, K.J. Thorley, J.E. Anthony, R. Bittl, R.H. Friend, A. Rao, N.C. Greenham, J. Behrends, Strongly exchange-coupled triplet pairs in an organic semiconductor, Nat. Phys. 13 (2017) 176–181, https://doi.org/10.1038/nphys3908.
[19] M.J. Tayebjee, S.N. Sanders, E. Kumarasamy, L.M. Campos, M.Y. Sfeir, D.R. McCamey, Quintet multiexciton dynamics in singlet fission, Nat. Phys. 13 (2) (2017) 182–188, https://doi.org/10.1038/nphys3909.
[20] Y.J. Bae, X. Zhao, M.D. Krzyaniak, H. Nagashima, J. Strzalka, Q. Zhang, M.R. Wasielewski, Spin dynamics of quintet and triplet states resulting from singlet fission in oriented terrylenediimide and quaterrylenediimide films, J. Phys. Chem. C 124 (2020) 9822–9833, https://doi.org/10.1021/acs.jpcc.0c03189.
[21] T. Ogiwara, Y. Wakikawa, T. Ikoma, Mechanism of intersystem crossing of thermally activated delayed fluorescence molecules, J. Phys. Chem. A 119 (14) (2015) 3415–3418, https://doi.org/10.1021/acs.jpca.5b02253.
[22] E.W. Evans, Y. Olivier, Y. Puttisong, W.K. Myers, T.J.H. Hele, S.M. Menke, T.H. Thomas, D. Credgington, D. Beljonne, R.H. Friend, N.C. Greenham, Vibrationally assisted Intersystem Crossing in benchmark thermally activated delayed fluorescence molecules, J. Phys. Chem. Lett. 9 (2018) 4053–4058, https://doi.org/10.1021/acs.jpclett.8b01556.
[23] B.H. Drummond, N. Aizawa, Y. Zhang, W.K. Myers, Y. Xiong, M.W. Cooper, S. Barlow, Q. Gu, L.R. Weiss, A.J. Gillett, D. Credgington, Y.-J. Pu, S.R. Marder, E.W.

Evans, Electron spin resonance resolves intermediate triplet states in delayed fluorescence, Nat. Commun. 12 (2021) 4532-1–4532-11, https://doi.org/10.1038/s41467-021-24612-9.
[24] M. Di Valentin, M. Albertini, E. Zurlo, M. Gobbo, D. Carbonera, The porphyrin triplet state as potential spin label for nanometer distance measurements by PELDOR spectroscopy, J. Am. Chem. Soc. 136 (2014) 6582–6585, https://doi.org/10.1021/ja502615n.
[25] C. Hintze, D. Bücker, S. Domingo Köhler, G. Jeschke, M. Drescher, Laser-Induced Magnetic Dipole Spectroscopy, J. Phys. Chem. Lett. just accep (2016), https://doi.org/10.1021/acs.jpclett.6b00765, acs.jpclett.6b00765.
[26] A. Bieber, M. Drescher, Light-induced dipolar spectroscopy – A quantitative comparison between LiDEER and LaserIMD, J. Magn. Reson. 296 (2018) 29–35, https://doi.org/10.1016/j.jmr.2018.08.006.
[27] A. Bertran, K.B. Henbest, M. De Zotti, M. Gobbo, C.R. Timmel, M. Di Valentin, A. M. Bowen, Light-Induced Triplet-Triplet Electron Resonance spectroscopy, J. Phys. Chem. Lett. 12 (2021) 80–85, https://doi.org/10.1021/acs.jpclett.0c02884.
[28] D.D. Awschalom, R. Hanson, J. Wrachtrup, B.B. Zhou, Quantum technologies with optically interfaced solid-state spins, Nat. Photonics 12 (2018) 516–527, https://doi.org/10.1038/s41566-018-0232-2.
[29] S.L. Bayliss, D.W. Laorenza, P.J. Mintun, B.D. Kovos, D.E. Freedman, D.D. Awschalom, Optically addressable molecular spins for quantum information processing, Science 370 (2020) 1309–1312, https://doi.org/10.1126/science.abb9352.
[30] S.M. Harvey, M.R. Wasielewski, Photogenerated spin-correlated radical pairs: from photosynthetic energy transduction to quantum information science, J. Am. Chem. Soc. 143 (2021) 15508–15529, https://doi.org/10.1021/jacs.1c07706.
[31] M. Mayländer, S. Chen, E.R. Lorenzo, M.R. Wasielewski, S. Richert, Exploring photogenerated molecular quartet states as spin qubits and qudits, J. Am. Chem. Soc. 143 (2021) 7050–7058, https://doi.org/10.1021/jacs.1c01620.
[32] R.M. Jacobberger, Y. Qiu, M.L. Williams, M.D. Krzyaniak, M.R. Wasielewski, Using molecular design to enhance the coherence time of quintet multiexcitons generated by singlet fission in single crystals, J. Am. Chem. Soc. 144 (2022) 2276–2283, https://doi.org/10.1021/jacs.1c12414.
[33] M.D.E. Forbes, L.E. Jarocha, S. Sim, V.F. Tarasov, Time-Resolved Electron Paramagnetic Resonance spectroscopy: History, technique, and application to supramolecular and macromolecular chemistry, in: Advances in Physical Organic Chemistry, 1st Edition, Vol. 47, Elsevier Ltd., 2013, Ch. 1, pp. 1–83. http://dx.doi.org/10.1016/B978-0-12-407754-6.00001-6.
[34] S. Weber, Transient EPR, eMagRes 6 (2017) 255–270. http://dx.doi.org/10.1002/9780470034590.emrstm1509.
[35] T.-S. Lin, Electron spin echo spectroscopy of organic triplets, Chem. Rev. 84 (1) (1984) 1–15, https://doi.org/10.1021/cr00059a001.
[36] F. Lendzian, R. Bittl, W. Lubitz, Pulsed ENDOR of the photoexcited triplet states of bacteriochlorophyll a and of the primary donor P865 in reaction centers of Rhodobacter sphaeroides R-26, Photosynth. Res. 55 (1998) 189–197, https://doi.org/10.1023/A:1006030221445.
[37] C.E. Tait, P. Neuhaus, H.L. Anderson, C.R. Timmel, D. Carbonera, M. Di Valentin, HYSCORE on Photoexcited Triplet States, Appl. Magn. Reson. 46 (4) (2015) 389–409, https://doi.org/10.1007/s00723-014-0624-5.
[38] S. Richert, C.E. Tait, C.R. Timmel, Delocalization of photoexcited triplet states probed by transient EPR and hyperfine spectroscopy, J. Magn. Reson. 280 (2017) 103–116, https://doi.org/10.1016/j.jmr.2017.01.005.
[39] R. Bittl, S.G. Zech, Pulsed EPR spectroscopy on short-lived intermediates in Photosystem I, Biochim. Biophys. Acta 1507 (2001) 194–211, https://doi.org/10.1016/S0005-2728(01)00210-9.
[40] R. Carmieli, Q. Mi, A.B. Ricks, E.M. Giacobbe, S.M. Mickley, M.R. Wasielewski, Direct Measurement of Photoinduced Charge Separation Distances in Donor - Acceptor Systems for Artificial Photosynthesis Using OOP-ESEEM, J. Am. Chem. Soc. 131 (2009) 8372–8373, https://doi.org/10.1021/ja902864h.
[41] C.R. Timmel, C.E. Fursman, A.J. Hoff, P.J. Hore, Spin-correlated radical pairs: microwave pulse effects on lifetimes, electron spin echo envelope modulations, and optimum conditions for detection by electron spin echo spectroscopy, Chem. Phys. 226 (3) (1998) 271–283, https://doi.org/10.1016/S0301-0104(97)00283-8.
[42] N. Mizuochi, Y. Ohba, S. Yamauchi, A two-dimensional EPR nutation study on excited multiplet states of fullerene linked to a nitroxide radical, J. Phys. Chem. A 101 (34) (1997) 5966–5968, https://doi.org/10.1021/jp971569y.
[43] S. Stoll, R.D. Britt, General and efficient simulation of pulse EPR spectra, Phys. Chem. Chem. Phys. 11 (31) (2009) 6614–6625, https://doi.org/10.1039/b907277b.
[44] P.J. Hore, D.A. Hunter, C.D. McKie, A.J. Hoff, Electron Paramagnetic Resonance of spin-correlated radical pairs in photosynthetic reactions, Chem. Phys. Lett. 137 (1987) 495–500, https://doi.org/10.1016/0009-2614(87)80617-6.
[45] R. Bittl, G. Kothe, Transient EPR of radical pairs in photosynthetic reaction centers: prediction of quantum beats, Chem. Phys. Lett. 177 (1991) 547–553, https://doi.org/10.1016/0009-2614(91)90082-K.
[46] P. Jaegermann, M. Plato, B. Von Maltzan, K. Möbius, Time-resolved EPR study of exciton hopping in porphyrin dimers in their photoexcited triplet state, Mol. Phys. 78 (1993) 1057–1074, https://doi.org/10.1080/00268979300100691.
[47] G. Kothe, S. Weber, E. Ohmes, M.C. Thurnauer, J.R. Norris, Transient EPR of light-induced spin-correlated radical pairs: Manifestation of zero quantum coherence, J. Phys. Chem. 98 (1994) 2706–2712, https://doi.org/10.1021/j100061a031.
[48] K. Ishii, J.-I. Fujisawa, A. Adachi, S. Yamauchi, N. Kobayashi, General simulations of excited quartet spectra with electron-spin polarizations: the excited multiplet states of (tetraphenylporphinato)zinc(II) coordinated by p- or m-pyridyl nitronyl nitroxides, J. Am. Chem. Soc. 120 (1998) 3152–3158, https://doi.org/10.1021/ja973146f.
[49] U. Segre, L. Pasimeni, M. Ruzzi, Simulation of EPR and time resolved EPR lineshapes in partially ordered glasses, Spectrochim. Acta A 56 (2000) 265–271, https://doi.org/10.1016/S1386-1425(99)00237-1.
[50] M. Fuhs, G. Elger, A. Osintsev, A. Popov, H. Kurreck, K. Möbius, Multifrequency time-resolved EPR (9.5 GHz and 95 GHz) on covalently linked porphyrin-quinone model systems for photosynthetic electron transfer: Effect of molecular dynamics on electron spin polarization, Mol. Phys. 98 (2000) 1025–1040, https://doi.org/10.1080/00268970050052079.
[51] Y. Teki, S. Miyamoto, M. Nakatsuji, Y. Miura, π-topology and spin alignment utilizing the excited molecular field: Observation of the excited high-spin quartet (S = 3/2) and quintet (S = 2) states on purely organic π-conjugated spin systems, J. Am. Chem. Soc. 123 (2001) 294–305, https://doi.org/10.1021/ja001920k.
[52] Y.E. Kandrashkin, A. Van Der Est, Electron spin polarization of the excited quartet state of strongly coupled triplet-doublet spin systems, J. Chem. Phys. 120 (2004) 4790–4799, https://doi.org/10.1063/1.1645773.
[53] A. Blank, H. Levanon, Triplet line shape simulation in continuous wave electron paramagnetic resonance experiments, Concept Magnetic Res. A 25 (2005) 18–39, https://doi.org/10.1002/cmr.a.20030.
[54] F. Kraffert, J. Behrends, Spin-correlated doublet pairs as intermediate states in charge separation processes, Mol. Phys. 115 (2017) 2373–2386, https://doi.org/10.1080/00268976.2016.1278479.
[55] Q. Mi, M.A. Ratner, M.R. Wasielewski, Time-Resolved EPR spectra of spin-correlated radical pairs: spectral and kinetic modulation resulting from electron-nuclear hyperfine interactions, J. Phys. Chem. A 114 (2010) 162–171, https://doi.org/10.1021/jp907476q.
[56] Q. Mi, M.A. Ratner, M.R. Wasielewski, Accurate and general solutions to three-dimensional anisotropies: Applications to EPR spectra of triplets involving dipole-dipole, spin-orbit interactions and liquid crystals, J. Phys. Chem. C 114 (2010) 13853–13860, https://doi.org/10.1021/jp103678m.
[57] Y. Kobori, M. Fuki, H. Murai, Electron spin polarization transfer to the charge-separated state from locally excited triplet configuration: theory and its application to characterization of geometry and electronic coupling in the electron donor-acceptor system, J. Phys. Chem. B 114 (2010) 14621–14630, https://doi.org/10.1021/jp102330a.
[58] T. Miura, R. Carmieli, M.R. Wasielewski, Time-Resolved EPR studies of charge recombination and triplet-state formation within donor - bridge - acceptor molecules having wire-like oligofluorene bridges, J. Phys. Chem. A 114 (2010) 5769–5778, https://doi.org/10.1021/jp101523n.
[59] S. Rein, Development of advanced analysis and simulation programs for EPR spectroscopy, Albert-Ludwigs-Universität Freiburg, 2019, Ph.D. thesis.
[60] S. Stoll, A. Schweiger, EasySpin, a comprehensive software package for spectral simulation and analysis in EPR, J. Magn. Reson. 178 (2006) 42–55, https://doi.org/10.1016/j.jmr.2005.08.013.
[61] T.J. Penfold, E. Gindensperger, C. Daniel, C.M. Marian, Spin-vibronic mechanism for Intersystem Crossing, Chem. Rev. 118 (2018) 6975–7025, https://doi.org/10.1021/acs.chemrev.7b00617.
[62] P.W. Atkins, Photochemical Processes, in: L.T. Muus, P.W. Atkins, K.A. McLauchlan, J.B. Pedersen (Eds.), Chemically Induced Magnetic Polarization. Nato Advanced Study Institutes Series, Springer, Dordrecht, 1977, Ch. X, pp. 181–190. http://dx.doi.org/10.1007/978-94-010-1265-2_10.
[63] B. Brocklehurst, K.A. McLauchlan, Free radical mechanism for the effects of environmental electromagnetic fields on biological systems, Int. J. Radiat. Biol. 69 (1996) 3–24, https://doi.org/10.1080/095530096146147.
[64] J.-P. Grivet, Electron Spin Resonance of phosphorescent anthracene, Chem. Phys. Lett. 4 (1969) 104–106, https://doi.org/10.1016/0009-2614(69)85082-7.
[65] D.A. Antheunis, J. Schmidt, J.H. van der Waals, Spin-forbidden radiationless processes in isoelectronic molecules: Anthracene, acridine and phenazine, Mol. Phys. 27 (1974) 1521–1541, https://doi.org/10.1080/00268977400101291.
[66] C.P.J. Poole, H.A. Farach, W.K. Jackson, Standardization of convention for zero field splitting parameters, J. Chem. Phys. 61 (1974) 2220–2221, https://doi.org/10.1063/1.1682294.
[67] M.C. Thurnauer, ESR study of the photoexcited triplet state in photosynthetic bacteria, Rev. Chem. Intermed. 3 (1979) 197–230, https://doi.org/10.1007/BF03052287.
[68] R.H. Clarke, H.A. Frank, Triplet state radiationless transitions in polycyclic hydrocarbons, J. Chem. Phys. 65 (1976) 39–47, https://doi.org/10.1063/1.432781.
[69] C.E. Tait, P. Neuhaus, H.L. Anderson, C.R. Timmel, Triplet state delocalization in a conjugated porphyrin dimer probed by transient Electron Paramagnetic Resonance techniques, J. Am. Chem. Soc. 137 (2015) 6670–6679, https://doi.org/10.1021/jacs.5b03249.
[70] Z.E.X. Dance, S.M. Mickley, T.M. Wilson, A.B. Ricks, A.M. Scott, M.A. Ratner, M. R. Wasielewski, Intersystem crossing mediated by photoinduced intramolecular charge transfer: Julolidine - Anthracene molecules with perpendicular pi systems, J. Phys. Chem. A 112 (2008) 4194–4201, https://doi.org/10.1021/jp800561g.
[71] M.L. Williams, I. Schlesinger, R.M. Jacobberger, M.R. Wasielewski, Mechanism of ultrafast triplet exciton formation in single cocrystals of π-stacked electron

donors and acceptors, J. Am. Chem. Soc. 144 (2022) 18607–18618, https://doi.org/10.1021/jacs.2c08584.
[72] A. Bencini, D. Gatteschi, Electron Paramagnetic Resonance of exchange-coupled systems, Springer, Heidelberg, 1990.
[73] T. Quintes, M. Mayländer, S. Richert, Properties and applications of photoexcited chromophore – radical systems, Nat. Rev. Chem. 7 (2023) 75–90, https://doi.org/10.1038/s41570-022-00453-y.
[74] K. Ishii, T. Ishizaki, N. Kobayashi, Experimental evidence for a selection rule of Intersystem Crossing to the excited quartet states: Metallophthalocyanines coordinated by 4-amino-TEMPO, J. Phys. Chem. A 103 (1999) 6060–6062, https://doi.org/10.1021/jp991293p.
[75] M.T. Colvin, E.M. Giacobbe, B. Cohen, T. Miura, A.M. Scott, M.R. Wasielewski, Competitive electron transfer and enhanced Intersystem Crossing in photoexcited covalent TEMPO - perylene-3,4:9,10-bis(dicarboximide) dyads: Unusual spin polarization resulting from the radical - triplet interaction, J. Phys. Chem. A 114 (2010) 1741–1748, https://doi.org/10.1021/jp909212c.
[76] E.M. Giacobbe, Q. Mi, M.T. Colvin, B. Cohen, C. Ramanan, A.M. Scott, S. Yeganeh, T.J. Marks, M.A. Ratner, M.R. Wasielewski, Ultrafast Intersystem Crossing and spin dynamics of linked to a nitroxide radical at fixed distances, J. Am. Chem. Soc. 131 (2009) 3700–3712, https://doi.org/10.1021/ja808924f.
[77] M.A. El-Sayed, D.S. Tinti, E.M. Yee, Conservation of spin direction and production of spin alignment in Triplet-Triplet Energy Transfer, J. Chem. Phys. 51 (1969) 5721–5723, https://doi.org/10.1063/1.1672008.
[78] H.C. Brenner, J.C. Brock, C.B. Harris, Energy Exchange in a Coherently Coupled Ensemble, Chem. Phys. 31 (1978) 137–164, https://doi.org/10.1016/0301-0104(78)87032-3.
[79] M.A. El-Sayed, Optical Pumping of the Lowest Triplet State and Multiple Resonance Optical Techniques in Zero Field, J. Chem. Phys. 54 (2) (1971) 680–691, https://doi.org/10.1063/1.1674896.
[80] K. Akiyama, S. Tero-Kubota, T. Ikoma, Y. Ikegami, Spin polarization conservation during intramolecular Triplet-Triplet Energy Transfer studied by Time-Resolved EPR spectroscopy, J. Am. Chem. Soc. 116 (1994) 5324–5327, https://doi.org/10.1021/ja00091a042.
[81] T. Imamura, Q. Onitsuka, H. Murai, K. Obi, Conservation of spin polarization during Triplet-Triplet Energy Transfer in low-temperature matrices, J. Phys. Chem. 88 (1984) 4028–4031, https://doi.org/10.1021/j150662a033.
[82] M. Di Valentin, C.E. Tait, E. Salvadori, S. Ceola, H. Scheer, R.G. Hiller, D. Carbonera, Conservation of spin polarization during triplet-triplet energy transfer in reconstituted peridinin-chlorophyll-protein complexes, J. Phys. Chem. B 115 (2011) 13371–13380, https://doi.org/10.1021/jp206978y.
[83] E. Hofmann, P.M. Wrench, F.P. Sharples, R.G. Hiller, W. Welte, K. Diederichs, Structural basis of light harvesting by carotenoids: Peridinin-Chlorophyll-Protein from Amphidinium carterae, Science 272 (1996) 1788–1791, https://doi.org/10.1126/science.272.5269.1788.
[84] S.K. Wong, D.A. Hutchinson, J.K.S. Wan, Chemically induced dynamic electron polarization. II.A general theory for radicals produced by photochemical reactions of excited triplet carbonyl compounds, J. Chem. Phys. 58 (1973) 985–989, https://doi.org/10.1063/1.1679355.
[85] P.J. Hore, Analysis of polarized EPR spectra, in: A.J. Hoff (Ed.), Advanced EPR - Applications in Biology and Biochemistry, Elsevier, 1989, Ch. 12, pp. 405–440. http://dx.doi.org/10.1016/B978-0-444-88050-5.50017-3.
[86] J.R. Norris, A.L. Morris, M.C. Thurnauer, J. Tang, A general model of electron spin polarization arising from the interactions within radical pairs, J. Chem. Phys. 92 (1990) 4239–4249, https://doi.org/10.1063/1.457782.
[87] S.A. Dzuba, P. Gast, A.J. Hoff, ESEEM study of spin-spin interactions in spin-polarized $P^{+}Q_{A}^{-}$ pairs in the photosynthetic purple bacterium Rhodobacter sphaeroides R26, Chem. Phys. Lett. 236 (1995) 595–602, https://doi.org/10.1016/0009-2614(95)00259-7.
[88] A.J. Hoff, P. Gast, S.A. Dzuba, C.R. Timmel, C.E. Fursman, P.J. Hore, The nuts and bolts of distance determination and zero- and double-quantum coherence in photoinduced radical pairs, Spectrochim. Acta A 54 (1998) 2283–2293, https://doi.org/10.1016/S1386-1425(98)00211-X.
[89] U. Ermler, G. Fritzsch, S.K. Buchanant, H. Michel, Structure of the photosynthetic reaction centre from Rhodobacter sphaeroides at 2.65 Åresolution: cofactors and protein-cofactor interactions, Structure 2 (1994) 925–936, https://doi.org/10.1016/S0969-2126(94)00094-8.
[90] T.F. Prisner, A. van der Est, R. Bittl, W. Lubitz, D. Stehlik, K. Möbius, Time-resolved W-band (95 GHz) EPR spectroscopy of Zn-substituted reaction centers of Rhodobacter sphaeroides R-26, Chem. Phys. 194 (1995) 361–370, https://doi.org/10.1016/0301-0104(95)00016-H.
[91] A. Van der Est, R. Bittl, E.C. Abresch, W. Lubitz, D. Stehlik, Transient EPR spectroscopy of perdeuterated Zn-substituted reaction centres of Rhodobacter sphaeroides R-26, Chem. Phys. Lett. 212 (1993) 561–568, https://doi.org/10.1016/0009-2614(93)85487-9.
[92] A. Van der Est, T.F. Prisner, R. Bittl, P. Fromme, W. Lubitz, K. Möbius, D. Stehlik, Time-resolved X-, K-, and W-Band EPR of the radical pair state $P_{700}^{\bullet+}$ $A_{1}^{\bullet-}$ of Photosystem I in comparison with $P_{865}^{\bullet+}$ $Q_{A}^{\bullet-}$ in bacterial reaction centers, J. Phys. Chem. B 101 (1997) 1437–1443, https://doi.org/10.1021/jp9622086.
[93] M. Di Valentin, A. Bisol, G. Agostini, M. Fuhs, P.A. Liddell, A.L. Moore, T.A. Moore, D. Gust, D. Carbonera, Photochemistry of artificial photosynthetic reaction centers in liquid crystals probed by multifrequency EPR (9.5 and 95 GHz), J. Am. Chem. Soc. 126 (51) (2004) 17074–17086, https://doi.org/10.1021/ja046067u.
[94] L. Pasimeni, L. Franco, M. Ruzzi, A. Mucci, L. Schenetti, C. Luo, D.M. Guldi, K. Kordatos, M. Prato, Evidence of high charge mobility in photoirradiated polythiophene-fullerene composites, J. Mater. Chem. 11 (2001) 981–983, https://doi.org/10.1039/b100842k.
[95] J. Behrends, A. Sperlich, A. Schnegg, T. Biskup, C. Teutloff, K. Lips, V. Dyakonov, R. Bittl, Direct detection of photoinduced charge transfer complexes in polymer fullerene blends, Phys. Rev. B 85 (2012) 125206-1–125206-6, https://doi.org/10.1103/PhysRevB.85.125206.
[96] Y. Kobori, T. Ako, S. Oyama, T. Tachikawa, K. Marumoto, Transient electron spin polarization imaging of heterogeneous charge-separation geometries at bulk-heterojunction interfaces in organic solar cells, J. Phys. Chem. C 123 (2019) 13472–13481, https://doi.org/10.1021/acs.jpcc.9b02672.
[97] J.H. Olshansky, J. Zhang, M.D. Krzyaniak, E.R. Lorenzo, M.R. Wasielewski, Selectively addressable photogenerated spin qubit pairs in DNA hairpins, J. Am. Chem. Soc. 142 (2020) 3346–3350, https://doi.org/10.1021/jacs.9b13398.
[98] M.B. Smith, J. Michl, Recent advances in singlet fission, Ann. Rev. Phys. Chem. 64 (2013) 361–386, https://doi.org/10.1146/annurev-physchem-040412-110130.
[99] B.S. Basel, J. Zirzlmeier, C. Hetzer, B.T. Phelan, M.D. Krzyaniak, S.R. Reddy, P.B. Coto, N.E. Horwitz, R.M. Young, F.J. White, F. Hampel, T. Clark, M. Thoss, R.R. Tykwinski, M.R. Wasielewski, D.M. Guldi, Unified model for singlet fission within a non-conjugated covalent pentacene dimer, Nat. Commun. 8 (2017) 15171-1–15171-8, https://doi.org/10.1038/ncomms15171.
[100] H. Nagashima, S. Kawaoka, S. Akimoto, T. Tachikawa, Y. Matsui, H. Ikeda, Y. Kobori, Singlet-fission-born quintet state: Sublevel selections and trapping by multiexciton thermodynamics, J. Phys. Chem. Lett. 9 (2018) 5855–5861, https://doi.org/10.1021/acs.jpclett.8b02396.
[101] M. Chen, M.D. Krzyaniak, J.N. Nelson, Y. Jue, S.M. Harvey, R.D. Schaller, R.M. Young, M.R. Wasielewski, Quintet-triplet mixing determines the fate of the multiexciton state produced by singlet fission in a terrylenediimide dimer at room temperature, Proc. Natl. Acad. Sci. 116 (2019) 8178–8183, https://doi.org/10.1073/pnas.1820932116.
[102] M.I. Collins, D.R. McCamey, M.J. Tayebjee, Fluctuating exchange interactions enable quintet multiexciton formation in singlet fission, J. Chem. Phys. 151 (2019) 164104-1–164104-8, https://doi.org/10.1063/1.5115816.
[103] Y. Kobori, M. Fuki, S. Nakamura, T. Hasobe, Geometries and terahertz motions driving quintet multiexcitons and ultimate triplet-triplet dissociations via the intramolecular singlet fissions, J. Phys. Chem. B 124 (2020) 9411–9419, https://doi.org/10.1021/acs.jpcb.0c07984.
[104] R.E. Merrifield, Magnetic effects on triplet exciton interactions, Pure Appl. Chem. 27 (1971) 481–498, https://doi.org/10.1351/pac197127030481.
[105] H. Benk, H. Sixl, Theory of two coupled triplet states application to bicarbene structures, Mol. Phys. 42 (1981) 779–801, https://doi.org/10.1080/00268978100100631.
[106] M. Wakasa, M. Kaise, T. Yago, R. Katoh, Y. Wakikawa, T. Ikoma, What can be learned from magnetic field effects on singlet fission: Role of exchange interaction in excited triplet pairs, J. Phys. Chem. C 119 (2015) 25840–25844, https://doi.org/10.1021/acs.jpcc.5b10176.
[107] S.L. Bayliss, L.R. Weiss, A. Mitioglu, K. Galkowski, Z. Yang, K. Yunusova, A. Surrente, K.J. Thorley, J. Behrends, R. Bittl, J.E. Anthony, A. Rao, R.H. Friend, P. Plochocka, P.C.M. Christianen, N.C. Greenham, A.D. Chepelianskii, Site-selective measurement of coupled spin pairs in an organic semiconductor, Proc. Natl. Acad. Sci. 115 (2018) 5077–5082, https://doi.org/10.1073/pnas.1718868115.
[108] M.C. Thurnauer, J.R. Norris, Magnetophotoselection applied to the triplet state observed by EPR in photosynthetic bacteria, Biochem. Biophys. Res. Commun. 73 (1976) 501–506, https://doi.org/10.1016/0006-291X(76)90735-X.
[109] A. Toffoletti, Z. Wang, J. Zhao, M. Tommasini, A. Barbon, Precise determination of the orientation of the transition dipole moment in a Bodipy derivative by analysis of the magnetophotoselection effect, Phys. Chem. Chem. Phys. 20 (2018) 20497–20503, https://doi.org/10.1039/c8cp01984c.
[110] I.V. Borovykh, I.I. Proskuryakov, I.B. Klenina, P. Gast, A.J. Hoff, Magnetophotoselection study of the lowest excited triplet state of the primary donor in photosynthetic bacteria, J. Phys. Chem. B 104 (2000) 4222–4228, https://doi.org/10.1021/jp993780a.
[111] A.J. Redman, G. Moise, S. Richert, E.J. Viere, W.K. Myers, M.J. Therien, C.R. Timmel, EPR of photoexcited triplet-state acceptor porphyrins, J. Phys. Chem. C 125 (2021) 11782–11790, https://doi.org/10.1021/acs.jpcc.1c03278.
[112] M.C. Thurnauer, J.R. Norris, The ordering of the zero field triplet spin sublevels in the chlorophylls. A magnetophotoselection study, Chem. Phys. Lett. 47 (1977) 100–105, https://doi.org/10.1016/0009-2614(77)85315-3.
[113] S. Ciuti, A. Agostini, A. Barbon, M. Bortolus, H. Paulsen, M.D. Valentin, D. Carbonera, Magnetophotoselection in the investigation of excitonically coupled chromophores: The case of the water-soluble chlorophyll protein, Molecules 27 (2022) 3654-1–3654-16, https://doi.org/10.3390/molecules27123654.
[114] T. Biskup, M. Sommer, S. Rein, D.L. Meyer, M. Kohlstädt, U. Würfel, S. Weber, Ordering of PCDTBT revealed by time-resolved Electron Paramagnetic Resonance spectroscopy of its triplet excitons, Angew. Chem. Int. Ed. 54 (2015) 7707–7710, https://doi.org/10.1002/anie.201502241.
[115] M. Di Valentin, E. Salvadori, S. Ceola, D. Carbonera, Pulsed EPR and ENDOR on the peridinin triplet state involved in the photoprotective mechanism in Peridinin-Chlorophyll a–Proteins, Appl. Magn. Reson. 37 (2009) 191–205, https://doi.org/10.1007/s00723-009-0046-y.

[116] W.G. van Dorp, W.H. Schoemaker, M. Soma, J.H. van der Waals, The lowest triplet state of free base porphin, Mol. Phys. 30 (1975) 1701–1721, https://doi.org/10.1080/00268977500103231.
[117] R.R. Ernst, G. Bodenhausen, A. Wokaun, Principles of Nuclear Magnetic Resonance in one and two dimensions, Clarendon Press, Oxford, 1987.
[118] J.H. Freed, J.B. Pedersen, The theory of chemically induced dynamic spin polarization, Adv. Magn. Opt. Reson. 8 (1976) 1–84, https://doi.org/10.1016/B978-0-12-025508-5.50006-2.
[119] M.R. Wasielewski, M.D.E. Forbes, N.L. Frank, K. Kowalski, G.D. Scholes, J. Yuen-Zhou, M.A. Baldo, D.E. Freedman, R.H. Goldsmith, T.I. Goodson, M.L. Kirk, J.K. McCusker, J.P. Ogilvie, D.A. Shultz, S. Stoll, K.B. Whaley, Exploiting chemistry and molecular systems for quantum information science, Nat. Rev. Chem. 4 (2020) 490–504, https://doi.org/10.1038/s41570-020-0200-5.